HHS Public Access

Author manuscript

*J Comp Neurol*. Author manuscript; available in PMC 2023 February 01.

Published in final edited form as:

*J Comp Neurol*. 2022 February ; 530(2): 537–552. doi:10.1002/cne.25228.

# The RNA-binding protein and stress granule component ATAXIN-2 is expressed in mouse and human tissues associated with glaucoma pathogenesis

**Chad A. Sundberg**[1,2], **Monika Lakk**[1], **Sharan Paul**[2], **Karla P. Figueroa**[2], **Daniel R. Scoles**[2], **Stefan M. Pulst**[2], **David Križaj**[1,3,4]

[1]Department of Ophthalmology & Visual Sciences, University of Utah, Salt Lake City, Utah, USA

[2]Department of Neurology, University of Utah, Salt Lake City, Utah, USA

[3]Department of Bioengineering, University of Utah, Salt Lake City, Utah, USA

[4]Department of Neurobiology & Anatomy, University of Utah, Salt Lake City, Utah, USA

## Abstract

Polyglutamine repeat expansions in the *Ataxin*-2 (*ATXN2*) gene were first implicated in Spinocerebellar Ataxia Type 2, a disease associated with degeneration of motor neurons and Purkinje cells. Recent studies linked single nucleotide polymorphisms in the gene to elevated intraocular pressure in primary open angle glaucoma (POAG); yet, the localization of ATXN2 across glaucoma-relevant tissues of the vertebrate eye has not been thoroughly examined. This study characterizes ATXN2 expression in the mouse and human retina, and anterior eye, using an antibody validated in ATXN2$^{-/-}$ retinas. ATXN2-ir was localized to cytosolic sub compartments in retinal ganglion cell (RGC) somata and proximal dendrites in addition to GABAergic, glycinergic, and cholinergic amacrine cells in the inner plexiform layer (IPL) and displaced amacrine cells. Human, but not mouse retinas showed modest immunolabeling of bipolar cells. ATXN2 immunofluorescence was prominent in the trabecular meshwork and pigmented and nonpigmented cells of the ciliary body, with analyses of primary human trabecular meshwork cells confirming the finding. The expression of ATXN2 in key POAG-relevant ocular tissues supports the potential role in autophagy and stress granule formation in response to ocular hypertension.

**Correspondence**: Stefan M. Pulst David Križaj, 65 N Mario Capecchi Drive, Bldg. 523, Room S4140, JMEC, Salt Lake City, UT 84132, USA. stefan.pulst@hsc.utah.edu; david.krizaj@hsc.utah.edu.

AUTHORS CONTRIBUTIONS

**Chad Sundberg, Monika Lakk, Sharan Paul, K.P. Figueroa, Daniel R. Scoles, Stefan M. Pulst, and David Križaj:** conceived and designed the experiments. **Chad Sundberg, Monika Lakk, Sharan Paul:** performed the experiments and analyzed the data. **Chad Sundberg, Monika Lakk, Sharan Paul, K.P. Figuero, Daniel R. Scoles, Stefan M. Pulst, and David Križaj:** wrote and edited the paper.

CONFLICT OF INTEREST

The authors declare that they have no known competing financial interests or personal relationships that could appear to influence the work reported in this study.

PERMISSION TO REPRODUCE MATERIALS FROM OTHER SOURCES

No third-party materials have been reproduced within this study.

PEER REVIEW

The peer review history for this article is available at https://publons.com/publon/10.1002/cne.25228.

**Keywords**

ATXN2; autophagy; primary open angle glaucoma; retinal ganglion cells; RNA-binding protein; SCA2; stress granules

## 1 | INTRODUCTION

Ataxin-2 (ATXN2), a ubiquitous 140 kDa RNA-binding protein composed of 1312 amino acids and a polyglutamine (polyQ) CAG repeat (Imbert et al., 1996; Pulst et al., 1996; Sanpei et al., 1996), promotes mRNA stability/translation, inhibits harmful miRNAs and noncoding RNA (ncRNA)-harboring R-loops within cytoplasmic translational complexes, and interacts with Src kinases, A2BP1/Fox1 splicing factors, and the ubiquitous nuclear riboprotein TDP-43 (Abraham et al., 2016; Drost et al., 2013; Elden et al., 2010; Fittschen et al., 2015; McCann et al., 2011; Shibata et al., 2000; Yokoshi et al., 2014). In vertebrates, ATXN2 is expressed in the developing and adult brain (cerebellar neurons and the olfactory bulb) and in the nonneuronal tissues such as heart, skeletal muscle, lung, liver, and gut (Huynh et al., 1999; Scoles et al., 2012). Its functions in healthy cells include mTOR (mechanistic target of rapamycin)-dependent nutrient sensing, calcium homeostasis, cytoskeletal organization, and endocytosis (Carmo-Silva et al., 2017; Halbach et al., 2017; Ostrowski et al., 2017; Satterfield et al., 2002), whereas stress periods induce assembly of ATXN2-containing stress granules composed of untranslated mRNAs and ribonuclear proteins within cytosolic stress granules and P-bodies (Figley et al., 2014; Nonhoff et al., 2007; Paul et al., 2018). Gain-of-function >33 poly-Q expansions in SCA2, ALS (amyotrophic lateral sclerosis), Parkinsonism patients and mutant mice have been associated with increased rates of stress granule formation, dysregulated $Ca^{2+}$ release from ER stores, TDP-43 proteinopathy, and neuronal loss (Huynh et al., 2003; Becker et al., 2017; Elden et al., 2010; Liu et al., 2009; Nonhoff et al., 2007; Paul et al., 2018; Scoles & Pulst, 2018; Watanabe et al., 2020). The prominent disease phenotypes include gait ataxia, muscle cramps and spasticity, cerebellar degeneration, nystagmus, slow saccadic eye movement, and frontal executive dysfunction (Scoles & Pulst, 2018), whereas mouse KO models and clinical trials for reduction of ATXN2 in SCA2/ALS showed reduced cell loss in vitro, reduced neuronal loss in vivo, and improved functional outcomes (Becker et al., 2017; Scoles et al., 2017). However, $Atxn2^{-/-}$ mice also show increased insulin production, decreased fertility, and deregulated lipid metabolism (Carmo-Silva et al., 2017; Lastres-Becker et al., 2008).

SCA2 patients may present with visual phenotypes such as retinal nerve fiber layer thinning, night blindness, ophthalmoparesis, ERG abnormalities, retinal dystrophy, and retinitis pigmentosa (Kurashige et al., 2020; Paciorkowski et al., 2011; Pula et al., 2011; Rufa et al., 2002; Volpe et al., 2015), whereas a recent GWAS study associated *ATXN2* SNPs with primary open angle glaucoma (POAG), a leading worldwide cause of irreversible blindness (Bailey et al., 2016; Jonas et al., 2017). Additional *ATXN2* polymorphisms have been linked to exfoliation glaucoma (Ma et al., 2019). Taking into account ocular phenotypes and pro-apoptotic impairment of autophagosome formation and stress granule clearance in glaucoma and ALS (Becker et al., 2017; Deluca et al., 2017; de Majo et al.,

2018; Fingert et al., 2017; Hirt & Liton, 2017; Kurashige et al., 2020; Paciorkowski et al., 2011; Paul et al., 2018; Porter et al., 2013; Pula et al., 2011; Rufa et al., 2002; Scoles et al., 2017; Volpe et al., 2015), it is conceivable that abnormal intracellular transport, translation, stability, and distribution of mRNAs in chronic ocular neuropathologies might involve ATXN2; yet, there is virtually no information about its ocular localization and expression. Here, we demonstrate strong ATXN2 expression in the somata and proximal dendrites of retinal ganglion cells (RGCs) and moderate ATXN2-ir signals in amacrine cells, horizontal cells, and the anterior eye, whereas retinal glia and ribbon synapse-containing neurons showed little expression. Our observations are consistent with ATXN2 functions in projection neurons, such as motor neurons and Purkinje cells, and identify ATXN2 as a potential target for functional studies and therapeutic assessment in the eye.

## 2 | RESULTS

### 2.1 | Ataxin-2 is predominantly localized to retinal ganglion cells

**2.1.1 | Mouse retina—**ATXN2 expression was investigated with a monoclonal antibody validated in previous characterizations of rodent central nervous system, heart, liver, and lower genito-urinary tract (Kiehl et al., 2006). Confocal fluorescent images of vertical sections of the wild-type mouse retina immunostained with the ATXN2 antibody showed prominent expression of the protein in RGCL (M = 29.350, $SD$ = 10.016) (Figure 1(a,b,f)), which was significantly decreased (t (190) = 12.788, $p < .0001$) in the Atxn2$^{-/-}$ retina (M = 14.447, $SD$ = 5.337) (Figure 1(c,d,f)). The normal organization of somatic and synaptic layers (Figure 1) in Atxn2$^{-/-}$ littermates (Figure 1(a)) indicates that ATXN2 is not required for retinal development and cell-type specification. Indicating specificity, the ATXN2 antibody recognized a single ~150 kDa band that was absent in *Atxn2*$^{-/-}$ retinas (Figure 1(e)). Co-staining with RBPMS (“RNA-binding protein with multiple splicing”) showed ATXN2 immunoreactivity (ir) in retinal ganglion cells (RGCs) (Figure 2(a,b)) in central, mid-peripheral, and peripheral retina (Figure 2(c–e)). Signals in large-diameter cells (white arrowheads) were more pronounced vis à vis smaller-diameter cells (yellow arrowheads in Figure 2(a,b,f–k)). ATXN2-ir was strongest in cell somata, with a subset of cells showing signal within the proximal dendrite (Figure 2(b)). Punctate cytoplasmic-nuclear expression agrees with proposed ATXN2 functions in transcription and formation of cytosolic translational complexes (Figley et al., 2014; Nonhoff et al., 2007; Paul et al., 2018; Yokoshi et al., 2014), whereas dendritic localization suggests the possibility of local translation (Eberwine et al., 2001; Kleiman et al., 1990). *Atxn2*$^{-/-}$ littermates (Figure 1(a)) showed normal organization of somatic and synaptic layers (Figure 1), suggesting that ATXN2 is not required for the retinal development and cell-type specification.

ATXN2-ir was also detected in the proximal inner plexiform layer (IPL) and nonRBPMS-ir cells within the RGCL (Figure 2(a,b)). To assess the potential localization to major amacrine subpopulations, retinas were double-labeled with choline acetyl transferase (ChAT; Figure 3(a–c)), glycine transferase 1 (GlyT1; Figure 3(d–f), and GAD 65/67 (Figure 3(g–i)) antibodies; horizontal cell (HC) expression was tested by double labeling with an anti-Calbindin D28k antibody (Figure 3(j,l)) (Krizaj et al., 2004; Ryskamp et al., 2011; Voinescu et al., 2009; Witkovsky et al., 2008). All three classes of amacrine cells from INL and GCL

regions were ATXN2-ir (yellow arrowheads in Figure 3). The overall signal intensity in INL and displaced amacrine cells was markedly weaker relative to RBPMS$^+$ cells (Figures 2 and 3(a–i)). Double labeling with calbindin (Figure 3(J–l)), a marker of axonbearing HCs in many species including mouse (Hamano et al., 1990), suggests moderate ATXN2 expression (Figures 3 and 4).

The retinal immunosignal was remarkable for cell types that did not express ATXN2. Photoreceptor somata in the outer nuclear layer (ONL) were consistently ATXN2-immunonegative, and the antibody did not indicate expression in bipolar cells based on colocalization with the pan-bipolar cell marker, OTX2 (not shown). Demonstrating lack of expression in retinal glia, ATXN2 did not colocalize with Müller cell (Figure 5(a–c,j–l)), microglial (Figure 5(g–i,p–r)), and astrocyte (Figure 5(d–f,m–o)) markers (glutamate synthase, IBA1, and GFAP, respectively) in mouse or human tissue). These data show that ATXN2 in the mouse retina is expressed in nonribbon-containing neurons with by far the strongest expression in RGCs but it is absent from glia, endothelial cells, and ribbon-containing neurons. Horizontal cells, which provide local/global feedforward and feedback signals to photoreceptors and bipolar cells through as-of-yet unknown synaptic mechanisms (Behrens et al., 2019 Preprint), are also ATXN2$^+$.

**2.1.2 | Human retina—**Immunohistochemical analysis in the human retina was conducted on tissue from two healthy donors (aged 76 and 78 years). ATXN2 signals matched the expression pattern seen in the mouse (Figures 1–4), with prominent ATXN2 immunoreactivity in RBPMS$^+$ cells (Figures 4(d–f) and 6(a–c)), and moderate levels of expression in GAD 65/67, GlyT1, and ChAT-labeled populations within the INL and GCL (Figure 6). Similar to mouse, ATXN2 was expressed in horizontal cells (Figure 6(d–f)); however, colocalization with OTX2 (Figure 6(g–i)) suggests potential expression in bipolar cells.

### 2.2 | ATXN2 is expressed in the trabecular meshwork and the ciliary body

**—**The pathogenesis of glaucoma has been linked to dysregulated autophagy mechanisms in trabecular meshwork (TM) cells that mediate the principal component of the outflow pathway (DeLuca et al., 2017; Fingert et al., 2017; Hirt & Liton, 2017; Nettesheim et al., 2019; Minegishi et al., 2016; Morton et al., 2008; Porter et al., 2014; Rezaie et al., 2002). The prominent ATXN2 immunoreactivity within the TM (Figure 7(d–i)), suggests that this may involve stress granules and/or ATXN2. The ATXN2 antibody labeled all three TM layers (corneoscleral, uveoscleral, and juxtacanalicular) but did not mark the endothelial cells that line the canal of Schlemm. We also examined ATXN2 signals in primary human TM cells isolated from healthy donors, which were ATXN2-ir (Figure 7(a–c)). Finally, ATXN2 expression was detected in nonpigmented and pigmented cells of the mouse (Figure 7(j–l)) and human ciliary body (Figure 7(m–o)), suggesting potential functions in regulation of aqueous humor secretion.

## 3 | DISCUSSION

This study was undertaken to ascertain the ocular distribution of ATXN2, a key intracellular stress-response protein that has been linked to multiple neurodegenerative diseases and

vision loss. We localized ATXN2 to anterior and posterior tissues of the mouse and human eye, including the retina, ciliary body, and the trabecular mesh-work. Arguing against a direct mechanistic link with ocular hypertension which initially targets RGCs and glia (Križaj, 2019; Krizaj et al., 2004), ATXN2 was also expressed in horizontal cells and displaced amacrine cells, which resist IOP stress (Harwerth et al., 2010; Kendell et al., 1995), but absent from glia, which function as early retinal responders to IOP (Inman and Horner, 2007; Woldemussie et al., 2004). The normal layering and structure in ATXN2$^{-/-}$ retinas suggest that the stress protein is not required for development or function in the healthy eye.

We found that the overall pattern of ATXN2 expression is largely conserved between mouse and human retinas. In the mouse, ATXN2 is expressed in three out of five classes of neuron, with dominant signals observed in spiking (RGCs and amacrine) cells whereas graded potential neurons (photoreceptors and bipolar cells) did not label for ATXN2. RGCs showed by far the strongest signal, with intense punctate immunofluorescence in somatic, perinuclear, and primary dendritic regions. Specifically, the RGC labeling pattern resembles cerebellar Purkinje cells (Huynh et al., 1999), in which cytosolic puncta were suggested to correspond to Golgi cisternae, ER cisternae, mitochondrial, nuclear and/or stress granule locations (Huynh et al., 2003; Ostrowski et al., 2017; van de Loo et al., 2009). The similarities in ATXN2 expression between RGCs and CNS/PNS projection neurons (Scoles & Pulst, 2018) suggest that the metabolic milieu in these cells requires localized and well-timed translation events.

The ATXN2 signal was expressed in every RBMPS$^{+}$ cell across central and peripheral regions. There was no evidence that ATXN2 is excluded from any RGC subtype (Duan et al., 2015; El-Danaf & Huberman, 2019), and the intensity of ATXN2-ir was the strongest in αRGC-like large-diameter cells. The somatic and dendritic signals in putative αRGCs suggest the possibility of compartmentalized stress signaling and mRNA processing at dendritic locations in a cell type that may be particularly vulnerable to mechanical and inflammatory injury (Guttenplan et al., 2020). ATXN2 functions in autophagy (Paul et al., 2018; Wardman et al., 2020) suggest possible links to TBK1 (tank-binding kinase 1) and OPT (optineurin) pathways that have been linked to impaired autophagosome formation and stress granule clearance in normotensive glaucoma, primary open angle glaucoma, SCA2, and ALS (de Majo et al., 2018; DeLuca et al., 2017; Fingert et al., 2017; Morton et al., 2008; Porter et al., 2013; Rezaie et al., 2002). RGC autophagy can be affected by acute and chronic IOP elevations (Deng et al., 2013; Park et al., 2012; Rodríguez-Muela et al., 2012; Su et al., 2014) with αRGCs responding with autophagic arrest, loss of synapses, and apoptosis (Della Santina et al., 2013; Guttenplan et al., 2020). While it remains to be seen whether manipulation of ocular ATXN2 reduces autophagic and apoptotic stress in hypertensive RGCs, it is worth noting that ATXN2 depletion is neuroprotective in SCA2 and ALS mouse models as well as ataxic flies (Auburger et al., 2017; Bakthavachalu et al., 2018; Becker et al., 2017; Lessing & Bonini, 2008; Scoles et al., 2017; Watanabe et al., 2020), possibly due to the loss of TDP-43 recruitment (Becker et al., 2017; Canet-Pons et al., 2021; Elden et al., 2010). It may also be of interest to determine potential ATXN2 colocalization with mTORC1 (mTOR, raptor, and S6 ribosomal proteins), which function as auxiliary nutrient sensors and autophagy suppressors in the inner retina, given their physical

interaction described in flies and modulatory activity described in mouse fibroblasts and human neuroblastoma cells (Lastres-Becker et al., 2016; Takahara & Maeda, 2012).

The predominant localization to spiking neurons suggests that ATXN2 signaling, stress granule formation, and quality control of nascent mRNAs might be associated with neuronal biosynthetic activity and cell firing patterns. We previously reported that ATXN2 repeat expansions interfere with stress granule assembly dynamics in Purkinje cells, leading to stress-granule-induced cytotoxicity and neurodegeneration in SCA2 and ALS (Huynh et al., 1999; Paul et al., 2018; Scoles et al., 2017). The similarity between the expression patterns in Purkinje cells and RGCs thus points at potential significance of non-ER mRNA signaling and stress granule assembly in projection neurons. Loss of TDP-43, a binding nuclear partner that is recruited by ATXN2 into stress granules (Becker et al., 2017; Canet-Pons et al., 2021; Elden et al., 2010; Kim et al., 2014), has been linked to retinal neurodegeneration, RGC axonal loss, and frontotemporal dementia (Atkinson et al., 2021; Ward et al., 2014; Watanabe et al., 2020). Depletion of ATXN2 has been shown to reduce TDP-43-mediated cytotoxicity (Becker et al., 2017) in Purkinje neurons, the predominant $ATXN2^{+}$ cell type in the cerebellum, which may suggest a similar treatment strategy for POAG may be effective.

Amacrine cells are the first neurons in the visual system to fire action potentials, with the three main subtypes (GABAergic; glycinergic and starburst), differing in stratification and dendritic arbor size (Diamond, 2017; Wässle et al., 2009; Yan et al., 2020). Similar to RGCs, amacrine cells utilize conventional synapses to transmit visual signals (Grimes et al., 2015), but in contrast to ganglion cells, nothing is known about autophagy or stress granule formation in these neurons. Our finding that ATXN2 is expressed in all three principal amacrine subtypes and therefore suggests novel functions for mRNA processing in these cells. Amacrine expression was modest compared to RGCs, potentially due to lower rates of firing and/or metabolic rates. In the mouse, ATXN2 was absent from photoreceptors and bipolar cells; however, its presence in HCs suggests an intriguing difference between retinal neurons that signal via graded membrane potentials, that is, ribbon-containing and nonribbon-containing graded-signaling neurons. Similar to the brain, the validated ATXN2 antibody (Huynh et al., 1999) labels glial subtypes (Müller cells, astrocytes and microglia) weakly, or indiscernibly from background immunofluorescence, whereas the nonexcitable cells in the anterior eye (ciliary body, trabecular meshwork, and corneal epithelial cells) were strongly immunopositive.

ATXN2 SNPs were associated with risk for contracting POAG (Bailey et al., 2016), an age-related disease associated with increased production of aqueous humor by the ciliary body or its decreased drainage via the trabecular meshwork (Križaj, 2019). Some studies (Ma et al., 2019) but not others (Aung et al., 2016), linked it to the exfoliation syndrome (XFS), a common risk factor for secondary glaucoma. Strong expression in the epithelial cells of the ciliary body (Figure 7) is in accord with the labeling of choroid plexus ependyma (Huynh et al., 1999) and other epithelia (Human Protein Atlas, n.d.; Lastres-Becker et al., 2019; Uhlén et al., 2015). Human TM tissue shows age- and IOP-dependent increases in the levels of autophagy markers (Pulliero et al., 2014) and autophagic flux in TM cells, as indicated by increased LC3-II/LC3-I ratio, and p-62, Beclin-1 and SMAD2 signaling in POAG and animal glaucoma models (Hirt & Liton, 2017; Nettesheim et al., 2020). In

vitro studies in porcine TM cells similarly showed increases in LC3-II following exposure to cyclic stretch (Porter et al., 2014). Because ATXN2 aggregation may be associated with increased levels of LC3-II and p62 (Paul et al., 2018), it may be of interest to determine whether intronic ATXN2 SNPs associated with POAG contribute to gradual accumulation of intracellular insults in the presence of relatively low increases in IOP. The association of ATXN2 mutations to pathological release from internal stores (Halbach et al., 2017), which play important roles in conventional outflow (Boussommier-Calleja et al., 2012; Rosenthal et al., 2005; Sumida & Stamer, 2011) additionally suggest functions in calcium homeostasis, mechanotransduction and trabecular function. The mechanosensitive channel TRPV4, which contributes to IOP regulation, is selectively localized to RGCs (Lakk et al., 2018; Ryskamp et al., 2011, 2016) and strongly expressed in the TM (Yarishkin et al., 2019, 2021) constitutes an element of the ATXN2 interactome together with the DDX1 protein associated with stress granule formation (Pérez-González et al., 2014).

## 4 | METHODS

### 4.1 | Animals

C57BL/6J mice (1–3 months of age) were obtained from JAX (Bar Harbor, ME). *Atxn2*−/− mice were generated as previously reported (Kiehl et al., 2006). The animals were maintained in a pathogen-free facility with a 12-hour light/dark cycle and ad libitum access to food and water at 22–23°C. No sex differences in the immunolabeling data were noted, so their data were pooled. Mice were euthanized by isoflurane and rapid cervical dislocation. The protocols were approved by the University of Utah Institutional Animal Care and Use Committee and adhered to the guidelines from Association for Research in Vision and Ophthalmology, Statement for the Use of Animals in Ophthalmic and Vision Research, and the US Public Health Service and Institute for Laboratory Animal Research.

### 4.2 | Human tissue

De-identified postmortem eyes from two donors (76-year-old male and 78-year-old female) with no history of glaucoma or other eye diseases were procured from Utah Lions Eye Bank with written informed consent of the donors' families. The maximum processing time was 3.5–4 h and the recovery protocols conformed to the standards set by the WMA Declaration of Helsinki and the Department of Health and Human Services Belmont Report. TM cells were isolated from juxtacanalicular and corneoscleral regions, as described (Yarishkin et al., 2018, 2021), in accordance with consensus characterization recommendations (Keller et al., 2018). Passage 2–4 TM cells were seeded onto Collagen I-seeded coverslips, grown in Trabecular Meshwork Cell Medium (ScienCell, Catalog#6591) at 37°C and 5% $CO_2$. The cell fixation and immunolabeling protocols were as reported (Lakk & Krizaj, 2020; Ryskamp et al., 2016).

### 4.3 | Immunohistochemistry

**4.3.1 | Vertical sections—**Mice were euthanized by isoflurane inhalation followed by cervical dislocation, after which eyes were enucleated and retinas fixed in 4% paraformaldehyde for 1 h, as described (Jo et al., 2017; Lakk et al., 2018). After wash (3 x 15 min) the tissue was dehydrated in 15% and 30% sucrose gradients for 12 h, embedded

in optimal cutting temperature (OCT) medium (Electron Microscopy Sciences, Hatfield, PA) and allowed to settle for 20 min then frozen on dry ice. Retinas were cryosectioned at 12 μm and stored at −20°C. Antibodies against known retinal cell markers were utilized (Table 1), with localization and labeling consistent with past reports (Jo et al., 2015, 2016, 2017; Lakk et al., 2018; Ryskamp et al., 2016). Cryosections were incubated in a blocking buffer (5% fetal bovine serum (FBS), 1% penicillin/streptomycin, and 0.3% Triton X-100 in 1x PBS) for 20–30 min. Sections were incubated in primary antibody buffer (2% bovine serum albumin (BSA), 1% penicillin/streptomycin, and 0.2% Triton X-100 in 1x PBS (phosphate buffer saline)) overnight at 4°C followed by incubation with fluorophore-conjugated secondary antibodies (1:500; goat anti-mouse AlexaFluor 405, 488 or 647, goat anti-rabbit AlexaFluor 488 or 594, Life Technologies/ThermoFisher, Carlsbad, CA) for 90 min at RT. ChAT bands were used to assess RGC dendritic stratification within the IPL.

**4.3.2 | Wholemount preparations—**Retinas were dissected in PBS, fixed in 4% PFA for 20 min and washed twice in PBS for 15 min. Retina were blocked in wholemount blocking buffer (4% BSA, 0.2% Triton X-100, and 1% penicillin/streptomycin) for 2 h and incubated with the primary antibody solution (2% BSA, 0.2% Triton X-100, and 1% penicillin/streptomycin) for 72 h at 4°C. Following the wash in sterile PBS (3x for 2 h), the tissue was incubated with fluorophore-conjugated secondary antibodies for 24 h and washed 3x for 2 h (6 h total). Images were acquired on an Olympus (Center Valley, PA) FV1200 confocal microscope using a 20x (N.A. water) objective. Images were processed and quantified with ImageJ (NIH; Bethesda, MD) (Rasband 1997-2018).

### 4.4 | Primary antibodies

**Ataxin-2—**(ATXN2) mouse antibody (BD Transduction Laboratories; RRID: AB_398900) was raised against the 713–904 amino acid sequence of the Human Ataxin-2 and purified from tissue culture supernatant by affinity chromatography. The manufacturer's data sheet shows it labels a ~150 kDa band and was tested by the manufacturer for reactivity against Human and Rat protein. The antibody has been characterized in the following publications (Boeynaems et al., 2017; Paul et al., 2018; Zhang et al., 2018) and fails to produce a Western blot band or a substantial immunofluorescence signal in Ataxin-2 knockout tissues (Figure 1).

**Ataxin-2—**(ATXN2) rabbit antibody was custom-designed against the EKSTESSSGPKREE epitope sequence common to both humans and mice (SCA2-280). Specific labelling for human and mouse peptide has been verified by Western blot and IHC in comparison to the previously listed commercial antibody and shown in previous publications (Hansen et al., 2013; Huynh et al., 1999; Nechiporuk et al., 1998).

**RNA binding protein with multiple splicing—**(RBPMS) antibody (Phosphosolutions; RRID: AB_2492225) was raised against a synthetic N-terminal peptide of the rat RBPMS sequence. The manufacturer's data sheet shows it labels a single band at ~24 kDa. We (Lakk et al., 2018) and others (Cueva Vargas et al., 2015; Johnson et al., 2019) previously showed that it colocalizes with Brn3a and selectively labels RGCs.

**Glial Fibrillary Acidic Protein—**(GFAP) antibody (Dako; RRID: AB_10013382) was raised against GFAP protein isolated from cow spinal cord. The cow protein shows between 90% and 95% homology with the human peptide and the manufacturer demonstrated reactivity by immunohistochemistry. GFAP is predominantly specific to astrocytes and undergoes marked upregulation following neuronal tissue injuries, selective labelling has been described previously by us (Jo et al., 2015) and others (Calbiague et al., 2020; Vessey et al., 2011).

**Glutamic Acid Decarboxylase—**(GAD-6) antibody (DSHB; AB_2314499) was raised against C-terminal sequence (a.a. 423–585) of purified protein from rat brain but it is reactive for mouse, human, and rat protein. The manufacturer's data sheet indicates it labels a single band at ~59 kDa. Verification for IHC has been described previously in our works (Ryskamp et al., 2011; Witkovsky et al., 2008) and the following publication (Lee et al., 2016).

**Glycine Transporter 1—**(GlyT1) antibody (Millipore; RRID: AB_90893) was raised in goat against synthetic C-terminal peptide from rat serum and has shown reactivity for mouse and human peptide. The antibody is specified for IHC and tested by the manufacturer against central nervous system tissues. It has been described in the following studies (Akopian et al., 2019; Gallagher et al., 2010; Voinescu et al., 2009).

**Choline acetyl transferase—**(ChAT) antibody (Millipore; RRID: AB_2079751) was raised in goat against the human placental peptide. According to manufacturer's data, it marks a ~70 kDa band on a Western blot of the mouse brain lysate. It labels the cholinergic (star-burst) amacrine cells in mouse and human retinas (Elshatory et al., 2007; Voinescu et al., 2009; Whitney et al., 2008).

**Calbindin D-28K—**(CALB) antibody (Millipore; RRID: AB_2068336) is a marker of axon-bearing HCs in mouse (Chua et al., 2013; Hamano et al., 1990; Krizaj et al., 2002). The antibody was raised in rabbit against recombinant mouse peptide with reactivity against human, mouse, and rat peptide based on significant sequence homology. A single Western blot product is detected at ~28 kDA.

**Orthodenticle homeobox 2—**(OTX2) antibody (R&D Systems; RRID: AB_2157172) derived from *Escherichia coli* against human Otx2 Met1-Leu289. Tested for specificity against human embryonic carcinoma cells and mouse embryo tissue and specificity has been shown in the following studies (Buenaventura et al., 2019; Yamamoto et al., 2020). The antibody labels a single Western product at ~37 kDa.

**Ionized calcium binding adaptor molecule 1—**(IBA1) antibody (Abcam; RRID: AB_2636859) was raised in rabbit with specificity against mouse, rat, and human protein and marks a single band at ~17 kDa. The antibody labels microglia specifically and has been used extensively in retinal studies (Cai et al., 2018; Hu et al., 2019; Kukreja et al., 2018).

**Glutamine synthetase—**(GS) antibody (Santa Cruz Biotechnology; RRID: AB_641095) was raised in goat against the C-terminal peptide of human origin and corresponds to a ~42

kDa Western blot product. The antibody shows reactivity with mouse and human peptide, among numerous other species, and is a specific marker for Müller glia in mouse and human retina (Bastone et al., 2009; Jager et al., 2020; Melzer et al., 2021).

## ACKNOWLEDGMENTS

The authors thank Kaylee Esparza Dayton, Megan Stricklin, and Christopher Nass Rudzitis for technical assistance and mouse handling. The authors also thank Dr. Ning Tian for the gift of the OTX2 antibody for recognition of bipolar cells.

### FUNDING INFORMATION

This work was funded by the following: National Institutes of Health (NEI: R01EY027920, R01EY031817, P30EY014800 D.K.; NINDS: R37NS033123, R56NS33123, R21NS10300 to S.M.P, R01NS097903 to D.R.S, U01NS103883 to S.M.P and D.R.S.), Glaucoma Research Foundation, Willard L. Eccles Foundation, ALSAM-Skaggs Foundation, the Neuroscience Initiative at the University of Utah and an Unrestricted Grant from Research to Prevent Blindness to the Department of Ophthalmology at the University of Utah (D.K.).

## DATA AVAILABILITY STATEMENT

Supporting data for this study is available from the corresponding author upon reasonable request.

## REFERENCES

Abraham KJ, Chan JN, Salvi JS, Ho B, Hall A, Vidya E, Guo R, Killackey SA, Liu N, Lee JE, Brown GW, & Mekhail K (2016). Intersection of calorie restriction and magnesium in the suppression of genome-destabilizing RNA-DNA hybrids. Nucleic Acids Research, 44(18), 8870–8884. 10.1093/nar/gkw752 [PubMed: 27574117]

Akopian A, Kumar S, Ramakrishnan H, Viswanathan S, & Bloomfield SA (2019). Amacrine cells coupled to ganglion cells via gap junctions are highly vulnerable in glaucomatous mouse retinas. The Journal of Comparative Neurology, 527(1), 159–173. 10.1002/cne.24074 [PubMed: 27411041]

Atkinson R, Leung J, Bender J, Kirkcaldie M, Vickers J, & King A (2021). TDP-43 mislocalization drives neurofilament changes in a novel model of TDP-43 proteinopathy. Disease Models & Mechanisms, 14(2), dmm047548. Advance online publication. 10.1242/dmm.047548

Auburger G, Sen NE, Meierhofer D, Başak AN, & Gitler AD (2017). Efficient prevention of neurodegenerative diseases by depletion of starvation response factor Ataxin-2. Trends in Neurosciences, 40(8), 507–516. 10.1016/j.tins.2017.06.004 [PubMed: 28684172]

Aung T, Ozaki M, Lee MC, Schlötzer-Schrehardt U, Thorleifsson G, Mizoguchi T, Igo RP, Haripriya A, Williams SE, Astakhov YS, Orr AC, Burdon KP, Nakano S, Mori K, Abu-Amero K, Hauser M, Li Z, Prakadeeswari G, Bailey JNC … Khor CC (2017). Genetic association study of exfoliation syndrome identifies a protective rare variant at LOXL1 and five new susceptibility loci. Nature Genetics, 49(7), 993–1004. 10.1038/ng.3875 [PubMed: 28553957]

Bailey JN, Loomis SJ, Kang JH, Allingham RR, Gharahkhani P, Khor CC, Burdon KP, Aschard H, Chasman DI, Igo RP, Hysi PG, Glastonbury CA, Ashley-Koch A, Brilliant M, Brown AA, Budenz DL, Buil A, Cheng CY, Choi H … Wiggs JL (2016). Genome-wide association analysis identifies TXNRD2, ATXN2 and FOXC1 as susceptibility loci for primary open-angle glaucoma. Nature Genetics, 48(2), 189–194. 10.1038/ng.3482 [PubMed: 26752265]

Bakthavachalu B, Huelsmeier J, Sudhakaran IP, Hillebrand J, Singh A, Petrauskas A, Thiagarajan D, Sankaranarayanan M, Mizoue L, Anderson EN, Pandey UB, Ross E, VijayRaghavan K, Parker R, & Ramaswami M (2018). RNP-granule assembly via Ataxin-2 disordered domains is required for long-term memory and neurodegeneration. Neuron, 98(4), 754–766.e4. 10.1016/j.neuron.2018.04.032 [PubMed: 29772202]

Bastone A, Fumagalli E, Bigini P, Perini P, Bernardinello D, Cagnotto A, Mereghetti I, Curti D, Salmona M, & Mennini T (2009). Proteomic profiling of cervical and lumbar spinal cord reveals

potential protective mechanisms in the wobbler mouse, a model of motor neuron degeneration. Journal of Proteome Research, 8(11), 5229–5240. 10.1021/pr900569d [PubMed: 19764823]

Becker LA, Huang B, Bieri G, Ma R, Knowles DA, Jafar-Nejad P, Messing J, Kim HJ, Soriano A, Auburger G, Pulst SM, Taylor JP, Rigo F, & Gitler AD (2017). Therapeutic reduction of ataxin-2 extends lifespan and reduces pathology in TDP-43 mice. Nature, 544(7650), 367–371. 10.1038/nature22038 [PubMed: 28405022]

Behrens C, Zhang Y, Yadav SC, Haverkamp S, Irsen S, Korympidou MM, Schaedler A, Dedek K, Smith RG, Euler T, Berens P, & Schubert T (2019). Retinal horizontal cells use different synaptic sites for global feedforward and local feedback signaling. bioRxiv. 10.1101/780031

Boeynaems S, Bogaert E, Kovacs D, Konijnenberg A, Timmerman E, Volkov A, Guharoy M, De Decker M, Jaspers T, Ryan VH, Janke AM, Baatsen P, Vercruysse T, Kolaitis RM, Daelemans D, Taylor JP, Kedersha N, Anderson P, Impens F … Van Den Bosch L (2017). Phase separation of C9orf72 dipeptide repeats perturbs stress granule dynamics. Molecular Cell, 65(6), 1044–1055.e5. 10.1016/j.molcel.2017.02.013 [PubMed: 28306503]

Boussommier-Calleja A, Bertrand J, Woodward DF, Ethier CR, Stamer WD, & Overby DR (2012). Pharmacologic manipulation of conventional outflow facility in ex vivo mouse eyes. Investigative Ophthalmology & Visual Science, 53(9), 5838–5845. 10.1167/iovs.12-9923 [PubMed: 22807298]

Buenaventura DF, Corseri A, & Emerson MM (2019). Identification of genes with enriched expression in early developing mouse cone photoreceptors. Investigative Ophthalmology & Visual Science, 60(8), 2787–2799. 10.1167/iovs.19-26951 [PubMed: 31260032]

Cai W, Feng D, Schwarzschild MA, McLean PJ, & Chen X (2018). Bimolecular fluorescence complementation of alpha-synuclein demonstrates its oligomerization with dopaminergic phenotype in mice. eBioMedicine, 29, 13–22. 10.1016/j.ebiom.2018.01.035 [PubMed: 29433982]

Calbiague VM, Vielma AH, Cadiz B, Paquet-Durand F, & Schmachtenberg O (2020). Physiological assessment of high glucose neurotoxicity in mouse and rat retinal explants. The Journal of Comparative Neurology, 528(6), 989–1002. 10.1002/cne.24805 [PubMed: 31674018]

Canet-Pons J, Sen NE, Arsović A, Almaguer-Mederos LE, Halbach MV, Key J, Döring C, Kerksiek A, Picchiarelli G, Cassel R, René F, Dieterlé S, Fuchs NV, König R, Dupuis L, Lütjohann D, Gispert S, & Auburger G (2021). Atxn2-CAG100-KnockIn mouse spinal cord shows progressive TDP43 pathology associated with cholesterol biosynthesis suppression. Neurobiology of Disease, 152, 105289. Advance online publication. 10.1016/j.nbd.2021.105289 [PubMed: 33577922]

Carmo-Silva S, Nobrega C, Pereira de Almeida L, & Cavadas C (2017). Unraveling the role of Ataxin-2 in metabolism. Trends in Endocrinology and Metabolism: TEM, 28(4), 309–318. 10.1016/j.tem.2016.12.006 [PubMed: 28117213]

Chua J, Nivison-Smith L, Fletcher EL, Trenholm S, Awatramani GB, & Kalloniatis M (2013). Early remodeling of Müller cells in the rd/rd mouse model of retinal dystrophy. The Journal of Comparative Neurology, 521(11), 2439–2453. 10.1002/cne.23307 [PubMed: 23348616]

Cueva Vargas JL, Osswald IK, Unsain N, Aurousseau MR, Barker PA, Bowie D, & Di Polo A (2015). Soluble tumor necrosis factor alpha promotes retinal ganglion cell death in Glaucoma via calcium-permeable AMPA receptor activation. *The Journal of Neuroscience*: The Official Journal of the Society for Neuroscience, 35(35), 12088–12102. 10.1523/JNEUROSCI.1273-15.2015

de Majo M, Topp SD, Smith BN, Nishimura AL, Chen HJ, Gkazi AS, Miller J, Wong CH, Vance C, Baas F, Ten Asbroek A, Kenna KP, Ticozzi N, Redondo AG, Esteban-Pérez J, Tiloca C, Verde F, Duga S, Morrison KE … Shaw CE (2018). ALS-associated missense and nonsense TBK1 mutations can both cause loss of kinase function. Neurobiology of Aging, 71, 266.e1–266.e10. 10.1016/j.neurobiolaging.2018.06.015

Della Santina L, Inman DM, Lupien CB, Horner PJ, & Wong RO (2013). Differential progression of structural and functional alterations in distinct retinal ganglion cell types in a mouse model of glaucoma. The Journal of Neuroscience: The Official Journal of the Society for Neuroscience, 33(44), 17444–17457. 10.1523/JNEUROSCI.5461-12.2013 [PubMed: 24174678]

DeLuca AP, Alward W, Liebmann J, Ritch R, Kawase K, Kwon YH, Robin AL, Stone EM, Scheetz TE, & Fingert JH (2017). Genomic organization of TBK1 copy number variations in Glaucoma patients. Journal of Glaucoma, 26(12), 1063–1067. 10.1097/IJG.0000000000000792 [PubMed: 28984711]

Deng S, Wang M, Yan Z, Tian Z, Chen H, Yang X, & Zhuo Y (2013). Autophagy in retinal ganglion cells in a rhesus monkey chronic hypertensive glaucoma model. PLoS One, 8(10), e77100. 10.1371/journal.pone.0077100 [PubMed: 24143204]

Diamond JS (2017). Inhibitory interneurons in the retina: Types, circuitry, and function. Annual Review of Vision Science, 3, 1–24. 10.1146/annurev-vision-102016-061345

Drost J, Nonis D, Eich F, Leske O, Damrath E, Brunt ER, Lastres-Becker I, Heumann R, Nowock J, & Auburger G (2013). Ataxin-2 modulates the levels of Grb2 and SRC but not ras signaling. Journal of Molecular Neuroscience: MN, 51(1), 68–81. 10.1007/s12031-012-9949-4 [PubMed: 23335000]

Duan X, Qiao M, Bei F, Kim IJ, He Z, & Sanes JR (2015). Subtype-specific regeneration of retinal ganglion cells following axotomy: Effects of osteopontin and mTOR signaling. Neuron, 85(6), 1244–1256. 10.1016/j.neuron.2015.02.017 [PubMed: 25754821]

Eberwine J, Miyashiro K, Kacharmina JE, & Job C (2001). Local translation of classes of mRNAs that are targeted to neuronal dendrites. Proceedings of the National Academy of Sciences of the United States of America, 98(13), 7080–7085. 10.1073/pnas.121146698 [PubMed: 11416191]

El-Danaf RN, & Huberman AD (2019). Sub-topographic maps for regionally enhanced analysis of visual space in the mouse retina. The Journal of Comparative Neurology, 527(1), 259–269. 10.1002/cne.24457 [PubMed: 29675855]

Elden AC, Kim HJ, Hart MP, Chen-Plotkin AS, Johnson BS, Fang X, Armakola M, Geser F, Greene R, Lu MM, Padmanabhan A, Clay-Falcone D, McCluskey L, Elman L, Juhr D, Gruber PJ, Rüb U, Auburger G, Trojanowski JQ … Gitler AD (2010). Ataxin-2 intermediate-length polyglutamine expansions are associated with increased risk for ALS. Nature, 466(7310), 1069–1075. 10.1038/nature09320 [PubMed: 20740007]

Elshatory Y, Everhart D, Deng M, Xie X, Barlow RB, & Gan L (2007). Islet-1 controls the differentiation of retinal bipolar and cholinergic amacrine cells. The Journal of Neuroscience: The Official Journal of the Society for Neuroscience, 27(46), 12707–12720. 10.1523/JNEUROSCI.3951-07.2007 [PubMed: 18003851]

Figley MD, Bieri G, Kolaitis RM, Taylor JP, & Gitler AD (2014). Profilin 1 associates with stress granules and ALS-linked mutations alter stress granule dynamics. The Journal of Neuroscience: The Official Journal of the Society for Neuroscience, 34(24), 8083–8097. 10.1523/JNEUROSCI.0543-14.2014 [PubMed: 24920614]

Fingert JH, Miller K, Hedberg-Buenz A, Roos BR, Lewis CJ, Mullins RF, & Anderson MG (2017). Transgenic TBK1 mice have features of normal tension glaucoma. Human Molecular Genetics, 26(1), 124–132. 10.1093/hmg/ddw372 [PubMed: 28025332]

Fittschen M, Lastres-Becker I, Halbach MV, Damrath E, Gispert S, Azizov M, Walter M, Müller S, & Auburger G (2015). Genetic ablation of ataxin-2 increases several global translation factors in their transcript abundance but decreases translation rate. Neurogenetics, 16(3), 181–192. 10.1007/s10048-015-0441-5 [PubMed: 25721894]

Gallagher SK, Witkovsky P, Roux MJ, Low MJ, Otero-Corchon V, Hentges ST, & Vigh J (2010). Beta-endorphin expression in the mouse retina. The Journal of Comparative Neurology, 518(15), 3130–3148. 10.1002/cne.22387 [PubMed: 20533364]

Grimes WN, Zhang J, Tian H, Graydon CW, Hoon M, Rieke F, & Diamond JS (2015). Complex inhibitory microcircuitry regulates retinal signaling near visual threshold. Journal of Neurophysiology, 114(1), 341–353. 10.1152/jn.00017.2015 [PubMed: 25972578]

Guttenplan KA, Stafford BK, El-Danaf RN, Adler DI, Münch AE, Weigel MK, Huberman AD, & Liddelow SA (2020). Neurotoxic reactive astrocytes drive neuronal death after retinal injury. Cell Reports, 31(12), 107776. 10.1016/j.celrep.2020.107776 [PubMed: 32579912]

Halbach MV, Gispert S, Stehning T, Damrath E, Walter M, & Auburger G (2017). Atxn2 knockout and CAG42-knock-in cerebellum shows similarly dysregulated expression in calcium homeostasis pathway. Cerebellum (London, England), 16(1), 68–81. 10.1007/s12311-016-0762-4

Hamano K, Kiyama H, Emson PC, Manabe R, Nakauchi M, & Tohyama M (1990). Localization of two calcium binding proteins, calbindin (28 kD) and parvalbumin (12 kD), in the vertebrate retina. The Journal of Comparative Neurology, 302(2), 417–424. 10.1002/cne.903020217 [PubMed: 2289978]

Hansen ST, Meera P, Otis TS, & Pulst SM (2013). Changes in Purkinje cell firing and gene expression precede behavioral pathology in a mouse model of SCA2. Human Molecular Genetics, 22(2), 271283. 10.1093/hmg/dds427

Harwerth RS, Wheat JL, Fredette MJ, & Anderson DR (2010). Linking structure and function in glaucoma. Progress in Retinal and Eye Research, 29(4), 249–271 10.1016/j.preteyeres.2010.02.001 [PubMed: 20226873]

Hirt J, & Liton PB (2017). Autophagy and mechanotransduction in outflow pathway cells. Experimental Eye Research, 158, 146–153. 10.1016/j.exer.2016.06.021 [PubMed: 27373974]

Hu Z, Deng N, Liu K, & Zeng W (2019). DLK mediates the neuronal intrinsic immune response and regulates glial reaction and neuropathic pain. Experimental Neurology, 322, 113056. 10.1016/j.expneurol.2019.113056 [PubMed: 31494101]

Human Protein Atlas. Available from http://www.proteinatlas.org

Huynh DP, Del Bigio MR, Ho DH, & Pulst SM (1999). Expression of ataxin-2 in brains from normal individuals and patients with Alzheimer's disease and spinocerebellar ataxia 2. Annals of Neurology, 45(2), 232–241. [PubMed: 9989626]

Huynh DP, Yang HT, Vakharia H, Nguyen D, & Pulst SM (2003). Expansion of the polyQ repeat in ataxin-2 alters its Golgi localization, disrupts the Golgi complex and causes cell death. Human Molecular Genetics, 12(13), 1485–1496. 10.1093/hmg/ddg175 [PubMed: 12812977]

Imbert G, Saudou F, Yvert G, Devys D, Trottier Y, Garnier JM, Weber C, Mandel JL, Cancel G, Abbas N, Durr A, Didierjean O, Stevanin G, Agid Y, & Brice A (1996). Cloning of the gene for spinocerebellar ataxia 2 reveals a locus with high sensitivity to expanded CAG/glutamine repeats. Nature Genetics, 14(3), 285–291. 10.1038/ng1196-285 [PubMed: 8896557]

Inman DM, & Horner PJ (2007). Reactive nonproliferative gliosis predominates in a chronic mouse model of glaucoma. Glia, 55(9), 942953. 10.1002/glia.20516.

Jager SE, Pallesen LT, Richner M, Harley P, Hore Z, McMahon S, Denk F, & Vaegter CB (2020). Changes in the transcriptional fingerprint of satellite glial cells following peripheral nerve injury. Glia, 68(7), 1375–1395. 10.1002/glia.23785 [PubMed: 32045043]

Jo AO, Lakk M, Frye AM, Phuong TT, Redmon SN, Roberts R, Berkowitz BA, Yarishkin O, & Križaj D (2016). Differential volume regulation and calcium signaling in two ciliary body cell types is subserved by TRPV4 channels. Proceedings of the National Academy of Sciences of the United States of America, 113(14), 3885–3890. 10.1073/pnas.1515895113 [PubMed: 27006502]

Jo AO, Noel JM, Lakk M, Yarishkin O, Ryskamp DA, Shibasaki K, McCall MA, & Križaj D (2017). Mouse retinal ganglion cell signalling is dynamically modulated through parallel anterograde activation of cannabinoid and vanilloid pathways. The Journal of Physiology, 595(20), 6499–6516. 10.1113/JP274562 [PubMed: 28766743]

Jo AO, Ryskamp DA, Phuong TT, Verkman AS, Yarishkin O, MacAulay N, & Križaj D (2015). TRPV4 and AQP4 channels synergistically regulate cell volume and calcium homeostasis in retinal Müller glia. The Journal of Neuroscience: The Official Journal of the Society for Neuroscience, 35(39), 13525–13537. 10.1523/JNEUROSCI.1987-15.2015 [PubMed: 26424896]

Johnson EN, Westbrook T, Shayesteh R, Chen EL, Schumacher JW, Fitzpatrick D, & Field GD (2019). Distribution and diversity of intrinsically photosensitive retinal ganglion cells in tree shrew. The Journal of Comparative Neurology, 527(1), 328–344. 10.1002/cne.24377 [PubMed: 29238991]

Jonas JB, Aung T, Bourne RR, Bron AM, Ritch R, & Panda-Jonas S (2017). Glaucoma. The Lancet, 390(10108), 2183–2193. 10.1016/s0140-6736(17)31469-1

Keller KE, Bhattacharya SK, Borrás T, Brunner TM, Chansangpetch S, Clark AF, Dismuke WM, Du Y, Elliott MH, Ethier CR, Faralli JA, Freddo TF, Fuchshofer R, Giovingo M, Gong H, Gonzalez P, Huang A, Johnstone MA, Kaufman PL, … Stamer WD (2018). Consensus recommendations for trabecular meshwork cell isolation, characterization and culture. Experimental Eye Research, 171, 164–173 10.1016/j.exer.2018.03.001 [PubMed: 29526795]

Kendell KR, Quigley HA, Kerrigan LA, Pease ME, & Quigley EN (1995). Primary open-angle glaucoma is not associated with photoreceptor loss. Investigative Ophthalmology & Visual Science, 36(1), 200–205. [PubMed: 7822147]

Kiehl TR, Nechiporuk A, Figueroa KP, Keating MT, Huynh DP, & Pulst SM (2006). Generation and characterization of Sca2 (ataxin-2) knockout mice. Biochemical and Biophysical Research Communications, 339(1), 17–24. 10.1016/j.bbrc.2005.10.186 [PubMed: 16293225]

Kim HJ, Raphael AR, LaDow ES, McGurk L, Weber RA, Trojanowski JQ, Lee VM, Finkbeiner S, Gitler AD, & Bonini NM (2014). Therapeutic modulation of eIF2α phosphorylation rescues TDP-43 toxicity in amyotrophic lateral sclerosis disease models. Nature Genetics, 46(2), 152–160. 10.1038/ng.2853 [PubMed: 24336168]

Kleiman R, Banker G, & Steward O (1990). Differential subcellular localization of particular mRNAs in hippocampal neurons in culture. Neuron, 5(6), 821–830. [PubMed: 2148488]

Križaj D (2019). What is glaucoma? In Kolb H, Nelson R, & Fernandez E (Eds.), Webvision: The organization of the retina and visual system. University of Utah Health Sciences Center.

Križaj D, Demarco SJ, Johnson J, Strehler EE, & Copenhagen DR (2002). Cell-specific expression of plasma membrane calcium ATPase isoforms in retinal neurons. The Journal of Comparative Neurology, 451(1), 1–21. 10.1002/cne.10281 [PubMed: 12209837]

Križaj D, Liu X, & Copenhagen DR (2004). Expression of calcium transporters in the retina of the tiger salamander *(Ambystoma tigrinum)*. The Journal of Comparative Neurology, 475(4), 463–480. 10.1002/cne.20170 [PubMed: 15236230]

Kukreja L, Shahidehpour R, Kim G, Keegan J, Sadleir KR, Russell T, Csernansky J, Mesulam M, Vassar RJ, Wang L, Dong H, & Geula C (2018). Differential neurotoxicity related to tetracycline Transactivator and TDP-43 expression in conditional TDP-43 mouse model of frontotemporal lobar degeneration. The Journal of Neuroscience: The Official Journal of the Society for Neuroscience, 38(27), 6045–6062. 10.1523/JNEUROSCI.1836-17.2018 [PubMed: 29807909]

Kurashige T, Morino H, Matsuda Y, Mukai T, Murao T, Toko M, Kume K, Ohsawa R, Torii T, Tokinobu H, Maruyama H, & Kawakami H (2020). Retinitis pigmentosa prior to familial ALS caused by a homozygous cilia and flagella-associated protein 410 mutation. Journal of Neurology, Neurosurgery, and Psychiatry, 91(2), 220–222. 10.1136/jnnp-2019-321279

Lakk M, & Križaj D (2020). Mechanotransduction in trabecular meshwork cells requires obligatory interactions between TRPV4 channels, rho signaling and focal adhesions. The FASEB Journal, 34, 1–1. 10.1096/fasebj.2020.34.s1.05782

Lakk M, Young D, Baumann JM, Jo AO, Hu H, & Križaj D (2018). Polymodal TRPV1 and TRPV4 sensors colocalize but do not functionally interact in a subpopulation of mouse retinal ganglion cells. Frontiers in Cellular Neuroscience, 12, 353. 10.3389/fncel.2018.00353 [PubMed: 30386208]

Lastres-Becker I, Brodesser S, Lütjohann D, Azizov M, Buchmann J, Hintermann E, Sandhoff K, Schümann A, Nowock J, & Auburger G (2008). Insulin receptor and lipid metabolism pathology in ataxin-2 knock-out mice. Human Molecular Genetics, 17(10), 14651481. 10.1093/hmg/ddn035

Lastres-Becker I, Nonis D, Eich F, Klinkenberg M, Gorospe M, Kötter P, Klein FA, Kedersha N, & Auburger G (2016). Mammalian ataxin-2 modulates translation control at the pre-initiation complex via PI3K/mTOR and is induced by starvation. Biochimica et Biophysica Acta, 1862(9), 1558–1569. 10.1016/j.bbadis.2016.05.017 [PubMed: 27240544]

Lastres-Becker I, Nonis D, Nowock J, & Auburger G (2019). New alternative splicing variants of the ATXN2 transcript. Neurological Research and Practice, 1, 22. 10.1186/s42466-019-0025-1 [PubMed: 33324888]

Lee SC, Weltzien F, Madigan MC, Martin PR, & Grünert U (2016). Identification of AII amacrine, displaced amacrine, and bistratified ganglion cell types in human retina with antibodies against calretinin. The Journal of Comparative Neurology, 524(1), 39–53. 10.1002/cne.23821 [PubMed: 26053777]

Lessing D, & Bonini NM (2008). Polyglutamine genes interact to modulate the severity and progression of neurodegeneration in Drosophila. PLoS Biology, 6(2), e29. 10.1371/journal.pbio.0060029 [PubMed: 18271626]

Liu J, Tang TS, Tu H, Nelson O, Herndon E, Huynh DP, Pulst SM, & Bezprozvanny I (2009). Deranged calcium signaling and neurodegeneration in spinocerebellar ataxia type 2. The Journal of Neuroscience: The Official Journal of the Society for Neuroscience, 29(29), 9148–9162. 10.1523/JNEUROSCI.0660-09.2009 [PubMed: 19625506]

Ma YN, Xie TY, & Chen XY (2019). Multiple gene polymorphisms associated with exfoliation syndrome in the Uygur population. Journal of Ophthalmology, 2019, 9687823. 10.1155/2019/9687823 [PubMed: 31192002]

McCann C, Holohan EE, Das S, Dervan A, Larkin A, Lee JA, Rodrigues V, Parker R, & Ramaswami M (2011). The Ataxin-2 protein is required for microRNA function and synapse-specific long-term olfactory habituation. Proceedings of the National Academy of Sciences of the United States of America, 108(36), E655–E662. 10.1073/pnas.1107198108 [PubMed: 21795609]

Melzer L, Freiman TM, & Derouiche A (2021). Rab6A as a Pan-astrocytic marker in mouse and human brain, and comparison with other glial markers (GFAP, GS, Aldh1L1, SOX9). Cell, 10(1), 72. 10.3390/cells10010072

Minegishi Y, Nakayama M, Iejima D, Kawase K, & Iwata T (2016). Significance of optineurin mutations in glaucoma and other diseases. Progress in Retinal and Eye Research, 55, 149–181. 10.1016/j.preteyeres.2016.08.002. [PubMed: 27693724]

Morton S, Hesson L, Peggie M, & Cohen P (2008). Enhanced binding of TBK1 by an optineurin mutant that causes a familial form of primary open angle glaucoma. FEBS Letters, 582(6), 997–1002. 10.1016/j.febslet.2008.02.047 [PubMed: 18307994]

Nechiporuk T, Huynh DP, Figueroa K, Sahba S, Nechiporuk A, & Pulst SM (1998). The mouse SCA2 gene: cDNA sequence, alternative splicing and protein expression. Human Molecular Genetics, 7(8), 1301–1309. 10.1093/hmg/7.8.1301 [PubMed: 9668173]

Nettesheim A, Dixon A, Shim MS, Coyne A, Walsh M, & Liton PB (2020). Autophagy in the aging and experimental ocular hypertensive mouse model. Investigative Ophthalmology & Visual Science, 61(10), 31. 10.1167/iovs.61.10.31

Nettesheim A, Shim MS, Hirt J, & Liton PB (2019). Transcriptome analysis reveals autophagy as regulator of TGFβ/Smad-induced fibrogenesis in trabecular meshwork cells. Scientific Reports, 9(1), 16092. 10.1038/s41598-019-52627-2 [PubMed: 31695131]

Nonhoff U, Ralser M, Welzel F, Piccini I, Balzereit D, Yaspo ML, Lehrach H, & Krobitsch S (2007). Ataxin-2 interacts with the DEAD/H-box RNA helicase DDX6 and interferes with P-bodies and stress granules. Molecular Biology of the Cell, 18(4), 1385–1396. 10.1091/mbc.e06-12-1120 [PubMed: 17392519]

Ostrowski LA, Hall AC, & Mekhail K (2017). Ataxin-2: From RNA control to human health and disease. Genes, 8(6), 157. 10.3390/genes8060157

Paciorkowski AR, Shafrir Y, Hrivnak J, Patterson MC, Tennison MB, Clark HB, & Gomez CM (2011). Massive expansion of SCA2 with autonomic dysfunction, retinitis pigmentosa, and infantile spasms. Neurology, 77(11), 1055–1060. 10.1212/WNL.0b013e31822e5627 [PubMed: 21880993]

Park HY, Kim JH, & Park CK (2012). Activation of autophagy induces retinal ganglion cell death in a chronic hypertensive glaucoma model. Cell Death & Disease, 3(4), e290. 10.1038/cddis.2012.26 [PubMed: 22476098]

Paul S, Dansithong W, Figueroa KP, Scoles DR, & Pulst SM (2018). Staufen1 links RNA stress granules and autophagy in a model of neurodegeneration. Nature Communications, 9(1), 3648. 10.1038/s41467-018-06041-3

Pérez-González A, Pazo A, Navajas R, Ciordia S, Rodriguez-Frandsen A, & Nieto A (2014). hCLE/C14orf166 associates with DDX1-HSPC117-FAM98B in a novel transcription-dependent shuttling RNA-transporting complex. PLoS One, 9(3), e90957. 10.1371/journal.pone.0090957 [PubMed: 24608264]

Porter K, Nallathambi J, Lin Y, & Liton PB (2013). Lysosomal basification and decreased autophagic flux in oxidatively stressed trabecular meshwork cells: Implications for glaucoma pathogenesis. Autophagy, 9(4), 581–594. 10.4161/auto.23568 [PubMed: 23360789]

Porter KM, Jeyabalan N, & Liton PB (2014). MTOR-independent induction of autophagy in trabecular meshwork cells subjected to biaxial stretch. Biochimica et Biophysica Acta, 1843(6), 1054–1062. 10.1016/j.bbamcr.2014.02.010 [PubMed: 24583119]

Pula JH, Towle VL, Staszak VM, Cao D, Bernard JT, & Gomez CM (2011). Retinal nerve fibre layer and macular thinning in spinocerebellar Ataxia and cerebellar multisystem atrophy. Neuroophthalmology (Aeolus Press), 35(3), 108–114. 10.3109/01658107.2011.580898

Pulliero A, Seydel A, Camoirano A, Saccà SC, Sandri M, & Izzotti A (2014). Oxidative damage and autophagy in the human trabecular meshwork as related with ageing. PLoS One, 9(6), e98106. 10.1371/journal.pone.0098106 [PubMed: 24945152]

Pulst SM, Nechiporuk A, Nechiporuk T, Gispert S, Chen XN, Lopes-Cendes I, Pearlman S, Starkman S, Orozco-Diaz G, Lunkes A, DeJong P, Rouleau GA, Auburger G, Korenberg JR, Figueroa C, & Sahba S (1996). Moderate expansion of a normally biallelic trinucleotide repeat in spinocerebellar ataxia type 2. Nature Genetics, 14(3), 269–276. 10.1038/ng1196-269 [PubMed: 8896555]

Rasband WS (1997-2018). ImageJ. U. S. National Institutes of Health, https://imagej.nih.gov/ij/

Rezaie T, Child A, Hitchings R, Brice G, Miller L, Coca-Prados M, Héon E, Krupin T, Ritch R, Kreutzer D, Crick RP, & Sarfarazi M (2002). Adult-onset primary open-angle glaucoma caused by mutations in optineurin. Science (New York, N.Y.), 295(5557), 1077–1079. 10.1126/science.1066901

Rodríguez-Muela N, Germain F, Mariño G, Fitze PS, & Boya P (2012). Autophagy promotes survival of retinal ganglion cells after optic nerve axotomy in mice. Cell Death and Differentiation, 19(1), 162–169. 10.1038/cdd.2011.88 [PubMed: 21701497]

Rosenthal R, Choritz L, Schlott S, Bechrakis NE, Jaroszewski J, Wiederholt M, & Thieme H (2005). Effects of ML-7 and Y-27632 on carbachol- and endothelin-1-induced contraction of bovine trabecular meshwork. Experimental Eye Research, 80(6), 837–845. 10.1016/j.exer.2004.12.013 [PubMed: 15939040]

Rufa A, Dotti MT, Galli L, Orrico A, Sicurelli F, & Federico A (2002). Spinocerebellar ataxia type 2 (SCA2) associated with retinal pigmentary degeneration. European Neurology, 47(2), 128–129. 10.1159/000047968 [PubMed: 11844906]

Ryskamp DA, Frye AM, Phuong TT, Yarishkin O, Jo AO, Xu Y, Lakk M, Iuso A, Redmon SN, Ambati B, Hageman G, Prestwich GD, Torrejon KY, & Križaj D (2016). TRPV4 regulates calcium homeostasis, cytoskeletal remodeling, conventional outflow and intraocular pressure in the mammalian eye. Scientific Reports, 6, 30583. 10.1038/srep30583 [PubMed: 27510430]

Ryskamp DA, Witkovsky P, Barabas P, Huang W, Koehler C, Akimov NP, Lee SH, Chauhan S, Xing W, Rentería RC, Liedtke W, & Krizaj D (2011). The polymodal ion channel transient receptor potential vanilloid 4 modulates calcium flux, spiking rate, and apoptosis of mouse retinal ganglion cells. The Journal of Neuroscience: The Official Journal of the Society for Neuroscience, 31(19), 7089–7101. 10.1523/JNEUROSCI.0359-11.2011 [PubMed: 21562271]

Sanpei K, Takano H, Igarashi S, Sato T, Oyake M, Sasaki H, Wakisaka A, Tashiro K, Ishida Y, Ikeuchi T, Koide R, Saito M, Sato A, Tanaka T, Hanyu S, Takiyama Y, Nishizawa M, Shimizu N, Nomura Y, … Tsuji S (1996). Identification of the spinocerebellar ataxia type 2 gene using a direct identification of repeat expansion and cloning technique, DIRECT. Nature Genetics, 14(3), 277–284. 10.1038/ng1196-277 [PubMed: 8896556]

Satterfield TF, Jackson SM, & Pallanck LJ (2002). A Drosophila homolog of the polyglutamine disease gene SCA2 is a dosage-sensitive regulator of Actin filament formation. Genetics, 162(4), 1687–1702. [PubMed: 12524342]

Scoles DR, Meera P, Schneider MD, Paul S, Dansithong W, Figueroa KP, Hung G, Rigo F, Bennett CF, Otis TS, & Pulst SM (2017). Antisense oligonucleotide therapy for spinocerebellar ataxia type 2. Nature, 544(7650), 362–366. 10.1038/nature22044 [PubMed: 28405024]

Scoles DR, Pflieger LT, Thai KK, Hansen ST, Dansithong W, & Pulst SM (2012). ETS1 regulates the expression of ATXN2. Human Molecular Genetics, 21(23), 5048–5065. 10.1093/hmg/dds349 [PubMed: 22914732]

Scoles DR, & Pulst SM (2018). Spinocerebellar Ataxia type 2. Advances in Experimental Medicine and Biology, 1049, 175–195. 10.1007/978-3-319-71779-1_8 [PubMed: 29427103]

Shibata H, Huynh DP, & Pulst SM (2000). A novel protein with RNA-binding motifs interacts with ataxin-2. Human Molecular Genetics, 9(9), 1303–1313. 10.1093/hmg/9.9.130 [PubMed: 10814712]

Su W, Li Z, Jia Y, & Zhuo Y (2014). Rapamycin is neuroprotective in a rat chronic hypertensive glaucoma model. PLoS One, 9(6), e99719. 10.1371/journal.pone.0099719 [PubMed: 24923557]

Sumida GM, & Stamer WD (2011). $S1P_2$ receptor regulation of sphingosine-1-phosphate effects on conventional outflow physiology. American Journal of Physiology Cell Physiology, 300(5), C1164–C1171. 10.1152/ajpcell.00437.2010 [PubMed: 21289286]

Takahara T, & Maeda T (2012). Transient sequestration of TORC1 into stress granules during heat stress. Molecular Cell, 47(2), 242–252. 10.1016/j.molcel.2012.05.019 [PubMed: 22727621]

Uhlén M, Fagerberg L, Hallström BM, Lindskog C, Oksvold P, Mardinoglu A, Sivertsson Å, Kampf C, Sjöstedt E, Asplund A, Olsson I, Edlund K, Lundberg E, Navani S, Szigyarto CA, Odeberg J, Djureinovic D, Takanen JO, Hober S, … Pontén F (2015). Proteomics. Tissue-based map of the human proteome. Science (New York, N.Y.), 347(6220), 1260419. 10.1126/science.1260419

van de Loo S, Eich F, Nonis D, Auburger G, & Nowock J (2009). Ataxin-2 associates with rough endoplasmic reticulum. Experimental Neurology, 215(1), 110–118. 10.1016/j.expneurol.2008.09.020 [PubMed: 18973756]

Vessey KA, Wilkinson-Berka JL, & Fletcher EL (2011). Characterization of retinal function and glial cell response in a mouse model of oxygen-induced retinopathy. The Journal of Comparative Neurology, 519(3), 506–527. 10.1002/cne.22530 [PubMed: 21192081]

Voinescu PE, Kay JN, & Sanes JR (2009). Birthdays of retinal amacrine cell subtypes are systematically related to their molecular identity and soma position. The Journal of Comparative Neurology, 517(5), 737–750. 10.1002/cne.22200 [PubMed: 19827163]

Volpe NJ, Simonett J, Fawzi AA, & Siddique T (2015). Ophthalmic manifestations of amyotrophic lateral sclerosis (an American ophthalmological society thesis). Transactions of the American Ophthalmological Society, 113, T12. [PubMed: 26877563]

Ward ME, Taubes A, Chen R, Miller BL, Sephton CF, Gelfand JM, Minami S, Boscardin J, Martens LH, Seeley WW, Yu G, Herz J, Filiano AJ, Arrant AE, Roberson ED, Kraft TW, Farese RV Jr., Green A, & Gan L (2014). Early retinal neurodegeneration and impaired ran-mediated nuclear import of TDP-43 in progranulin-deficient FTLD. The Journal of Experimental Medicine, 211(10), 1937–1945. 10.1084/jem.20140214 [PubMed: 25155018]

Wardman JH, Henriksen EE, Marthaler AG, Nielsen JE, & Nielsen TT (2020). Enhancement of autophagy and solubilization of Ataxin-2 alleviate apoptosis in spinocerebellar Ataxia type 2 patient cells. Cerebellum (London, England), 19(2), 165–181. 10.1007/s12311-019-01092-8

Wässle H, Heinze L, Ivanova E, Majumdar S, Weiss J, Harvey RJ, & Haverkamp S (2009). Glycinergic transmission in the mammalian retina. Frontiers in Molecular Neuroscience, 2, 6. 10.3389/neuro.02.006.2009 [PubMed: 19924257]

Watanabe R, Higashi S, Nonaka T, Kawakami I, Oshima K, Niizato K, Akiyama H, Yoshida M, Hasegawa M, & Arai T (2020). Intracellular dynamics of Ataxin-2 in the human brains with normal and frontotemporal lobar degeneration with TDP-43 inclusions. Acta Neuropathologica Communications, 8(1), 176. 10.1186/s40478-020-01055-9 [PubMed: 33115537]

Whitney IE, Keeley PW, Raven MA, & Reese BE (2008). Spatial patterning of cholinergic amacrine cells in the mouse retina. The Journal of Comparative Neurology, 508(1), 1–12. 10.1002/cne.21630 [PubMed: 18288692]

Witkovsky P, Gábriel R, & Krizaj D (2008). Anatomical and neurochemical characterization of dopaminergic interplexiform processes in mouse and rat retinas. The Journal of Comparative Neurology, 510(2), 158–174. 10.1002/cne.21784 [PubMed: 18615559]

Woldemussie E, Wijono M, & Ruiz G (2004). Müller cell response to laser-induced increase in intraocular pressure in rats. Glia, 47(2), 109119. 10.1002/glia.20000.

Yamamoto H, Kon T, Omori Y, & Furukawa T (2020). Functional and evolutionary diversification of Otx2 and Crx in vertebrate retinal photoreceptor and bipolar cell development. Cell Reports, 30(3), 658–671.e5. 10.1016/j.celrep.2019.12.072 [PubMed: 31968244]

Yan RS, Yang XL, Zhong YM, & Zhang DQ (2020). Spontaneous depolarization-induced action potentials of ON-starburst Amacrine cells during cholinergic and glutamatergic retinal waves. Cell, 9(12), 2574. 10.3390/cells9122574

Yarishkin O, Baumann JM, & Križaj D (2019). Mechano-electrical transduction in trabecular meshwork involves parallel activation of TRPV4 and TREK-1 channels. Channels (Austin, Tex.), 13(1), 168–171. 10.1080/19336950.2019.1618149

Yarishkin O, Phuong T, Baumann JM, De Ieso ML, Vazquez-Chona F, Rudzitis CN, Sundberg C, Lakk M, Stamer WD, & Križaj D (2021). Piezo1 channels mediate trabecular meshwork mechanotransduction and promote aqueous fluid outflow. The Journal of Physiology, 599(2), 571–592. 10.1113/JP281011 [PubMed: 33226641]

Yarishkin O, Phuong T, Bretz CA, Olsen KW, Baumann JM, Lakk M, Crandall A, Heurteaux C, Hartnett ME, & Križaj D (2018). TREK-1 channels regulate pressure sensitivity and calcium signaling in trabecular meshwork cells. The Journal of General Physiology, 150(12), 1660–1675. 10.1085/jgp.201812179 [PubMed: 30446509]

Yokoshi M, Li Q, Yamamoto M, Okada H, Suzuki Y, & Kawahara Y (2014). Direct binding of Ataxin-2 to distinct elements in 3′ UTRs promotes mRNA stability and protein expression. Molecular Cell, 55(2), 186–198. 10.1016/j.molcel.2014.05.022 [PubMed: 24954906]

Zhang K, Daigle JG, Cunningham KM, Coyne AN, Ruan K, Grima JC, Bowen KE, Wadhwa H, Yang P, Rigo F, Taylor JP, Gitler AD, Rothstein JD, & Lloyd TE (2018). Stress granule assembly disrupts nucleocytoplasmic transport. Cell, 173(4), 958–971.e17. 10.1016/j.cell.2018.03.025 [PubMed: 29628143]

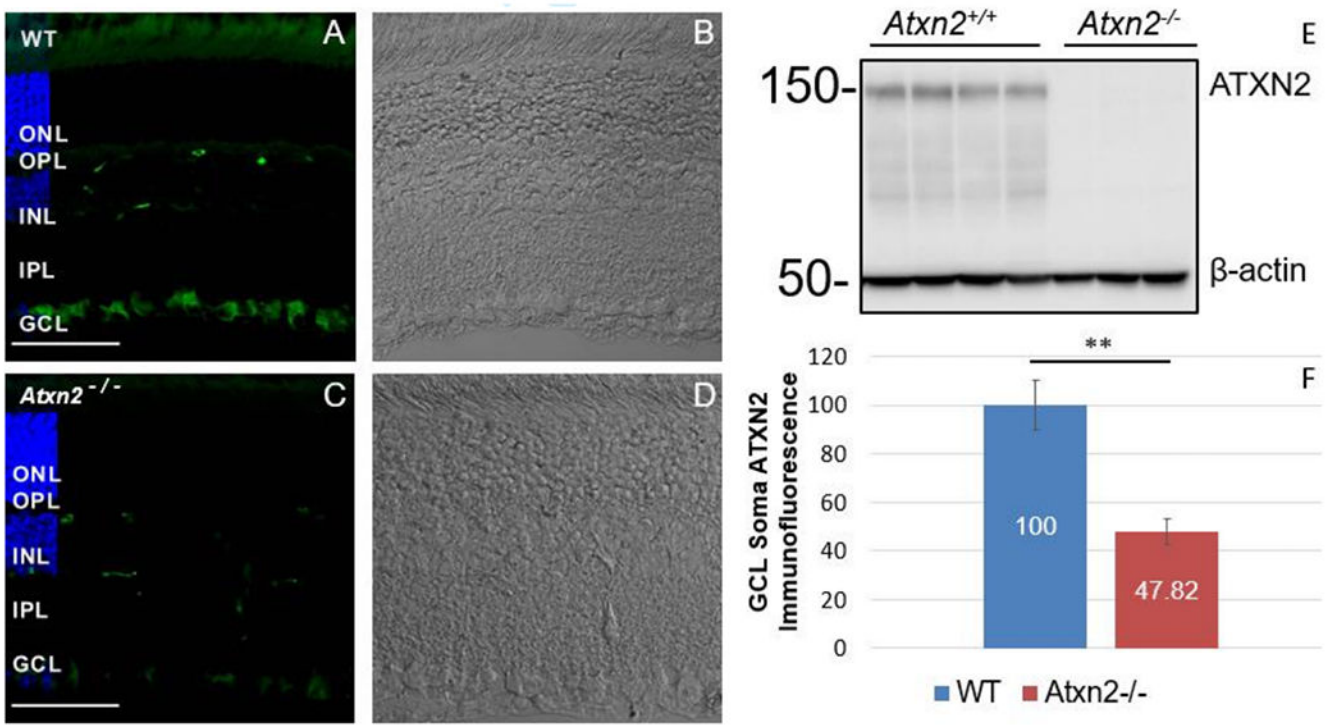


**FIGURE 1.**

Vertical sections of retinas from Atxn2$^{-/-}$ and age-matched wild-type littermate mice labeled for DAPI (insets, blue) and ATXN2 (green). (a, b) The majority of ATXN2 immunofluorescence in WT retinas (M = 29.350, *SD* = 10.016) localized to the ganglion cell layer. (c, d) Most of the signal is lost in Atxn2$^{-/-}$ retinas (M = 14.447, *SD* = 5.337). Brightfield images indicate normal retinal architecture. (e) ATXN2 protein expression was confirmed by Western blot for whole retina lysates from Atxn2$^{-/-}$ mice (*n* = 3) and age-matched wild-type littermates (*n* = 4) with β-actin utilized as an internal control. Scale bars = 25 μm. (f) RGCL ATXN2--ir quantified for wild type and KO retinal samples [Color figure can be viewed at wileyonlinelibrary.com]

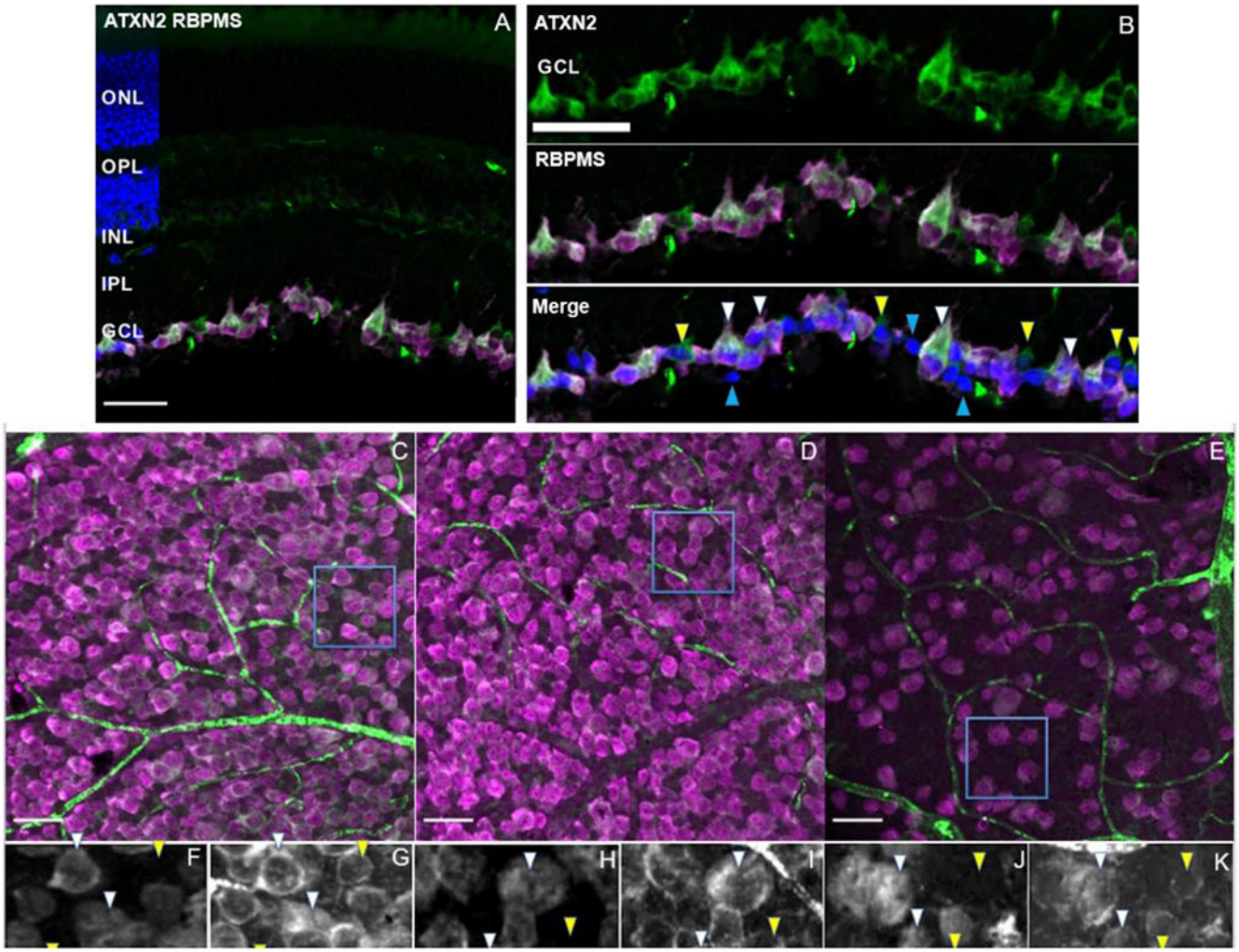


**FIGURE 2.**

(a) Immunoreactivity for ATXN2 (green) and the retinal ganglion cell (RGC)-specific marker, RNA binding protein with multiple splicing (RBPMS) (magenta) shows strong ATXN2-RBPMS colocalization in the RGCL. (b) RGCL detail. RGCs (RBPMS+ ATXN2+; white arrowheads) were strongly ATXN2-ir. Displaced amacrine cells (RBPMS−, ATXN2+; yellow arrowheads) showed modest ATXN2-ir whereas putative astroglial somata (blue arrowheads) were ATXN2-immunonegative. (c-k) Retina wholemounts immunostained for ATXN2 (green) and RBPMS (magenta). ATXN2 is localized to RGCs, and amacrine cells, in central (c), mid-peripheral (d), and peripheral retina (e) i. Insets in f-k show parallel RBPMS (f,h,j) and ATXN2 (g,i,k) channels for the respective wholemounts from central, mid-central, and peripheral retina. ATXN2 is expressed in amacrine cells (yellow arrowheads, ATXN2+, RBPMS− cells) and RGCs (white arrowheads, ATXN2+, RBPMS+ cells. Scale bars: 25 μm (a–e), 50 $\mu m^2$ (f–k) [Color figure can be viewed at wileyonlinelibrary.com]

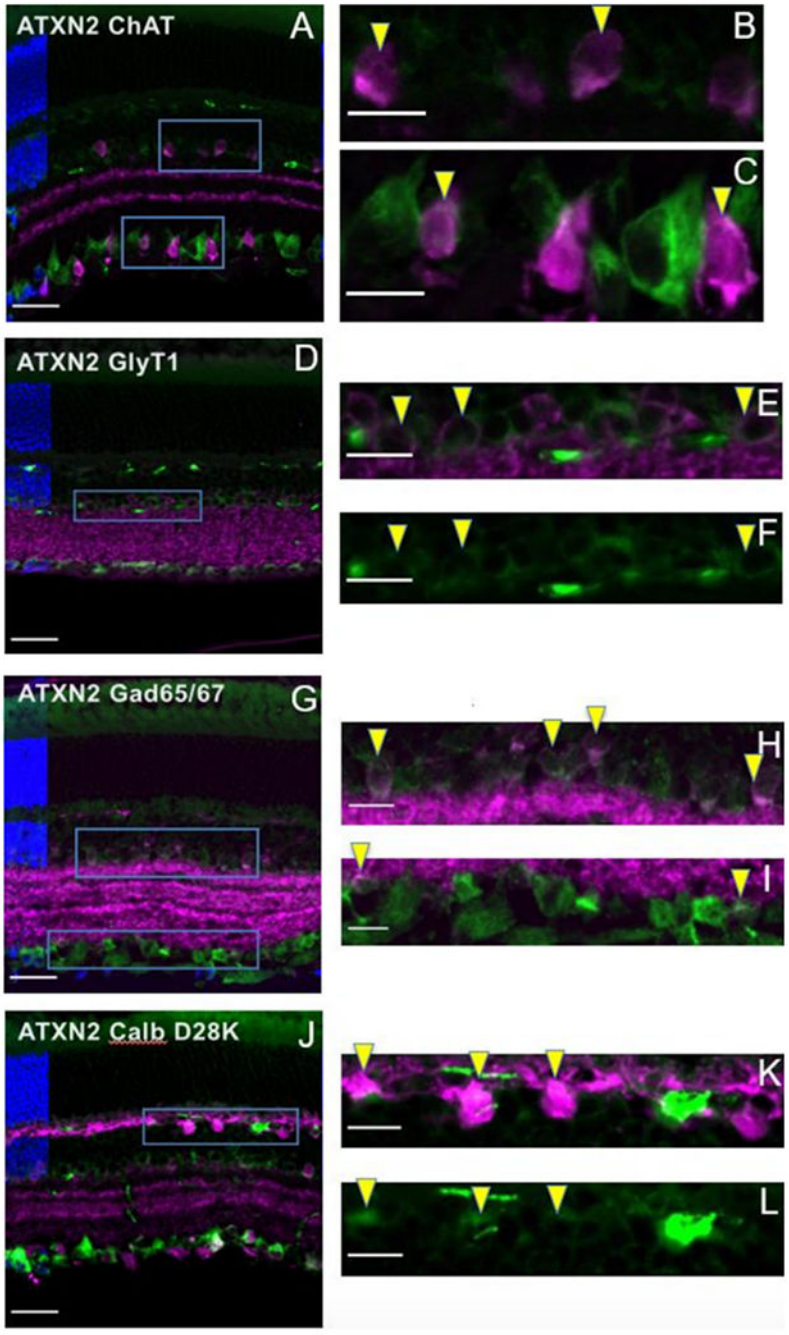


**FIGURE 3.**

Wild-type mouse retina vertical sections co-labeled for ATXN2 (green) and markers (magenta) for cholinergic amacrine cells (ChAT) (a–c), glycinergic amacrine cells (GlyT1) (d,f), and GABAergic amacrine cells (GAD66/67) (g,i). ATXN2-ir labeled all classes of amacrine cell. Co-localization between ATXN2 (green) and calbindin D28K (magenta) suggests expression in horizontal cells j–l). Scale bars: 25 μm (a,d,g,j) and 10 μm (b,c,e,f,h,i.k,l) [Color figure can be viewed at wileyonlinelibrary.com]

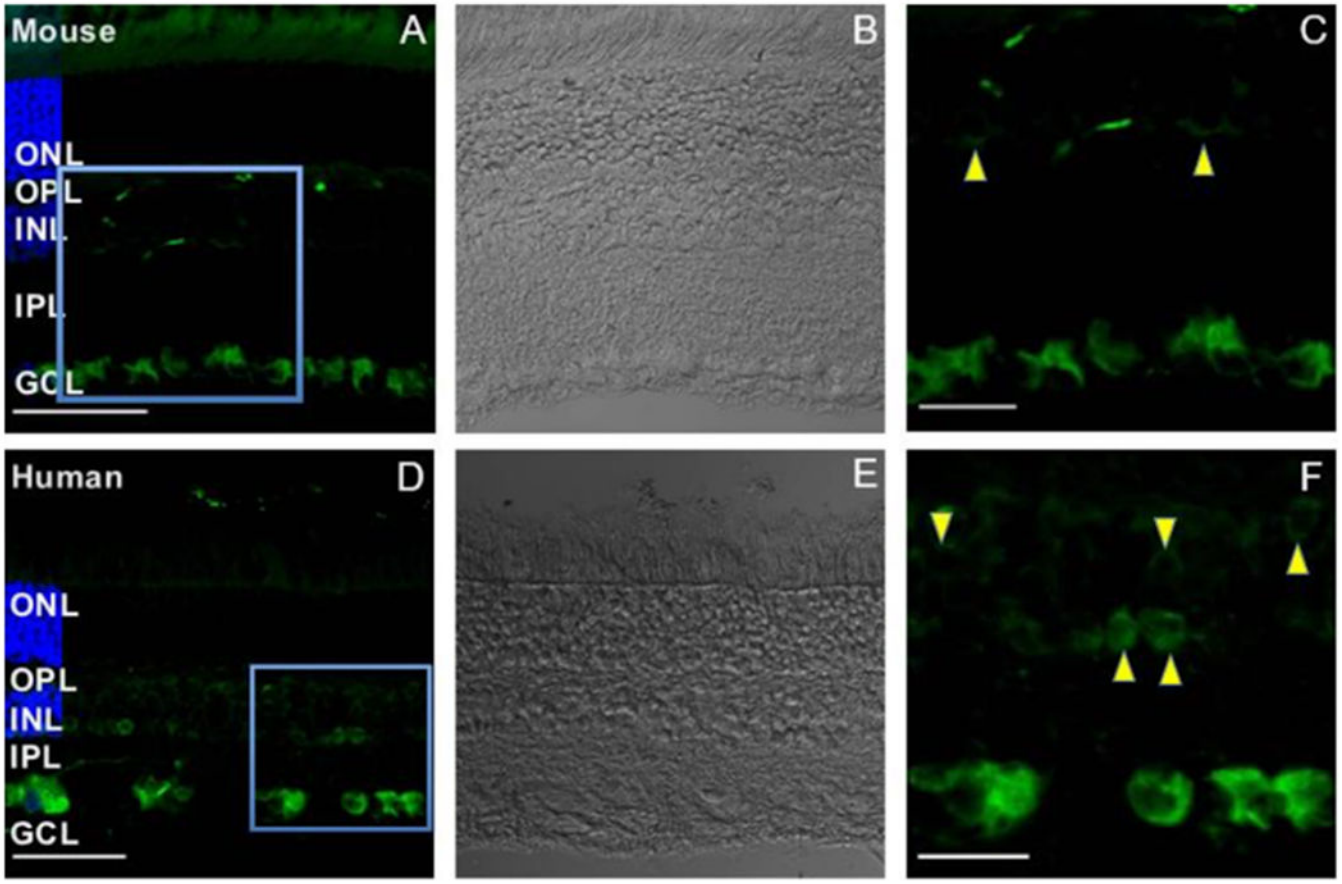


**FIGURE 4.**

Vertical sections from mouse (a–c) and human v(d–f) retinas labeled for ATXN2 (green) and DAPI (blue). The expression is remarkably similar apart from the ATXN2-ir in the human INL. Enlarged insets (c,f) indicate ATXN2-ir of INL (yellow arrowheads) in human vs. mouse tissue. Scale bars: 25 μm (a,b,d,e) and 10 μm (c,f) [Color figure can be viewed at wileyonlinelibrary.com]

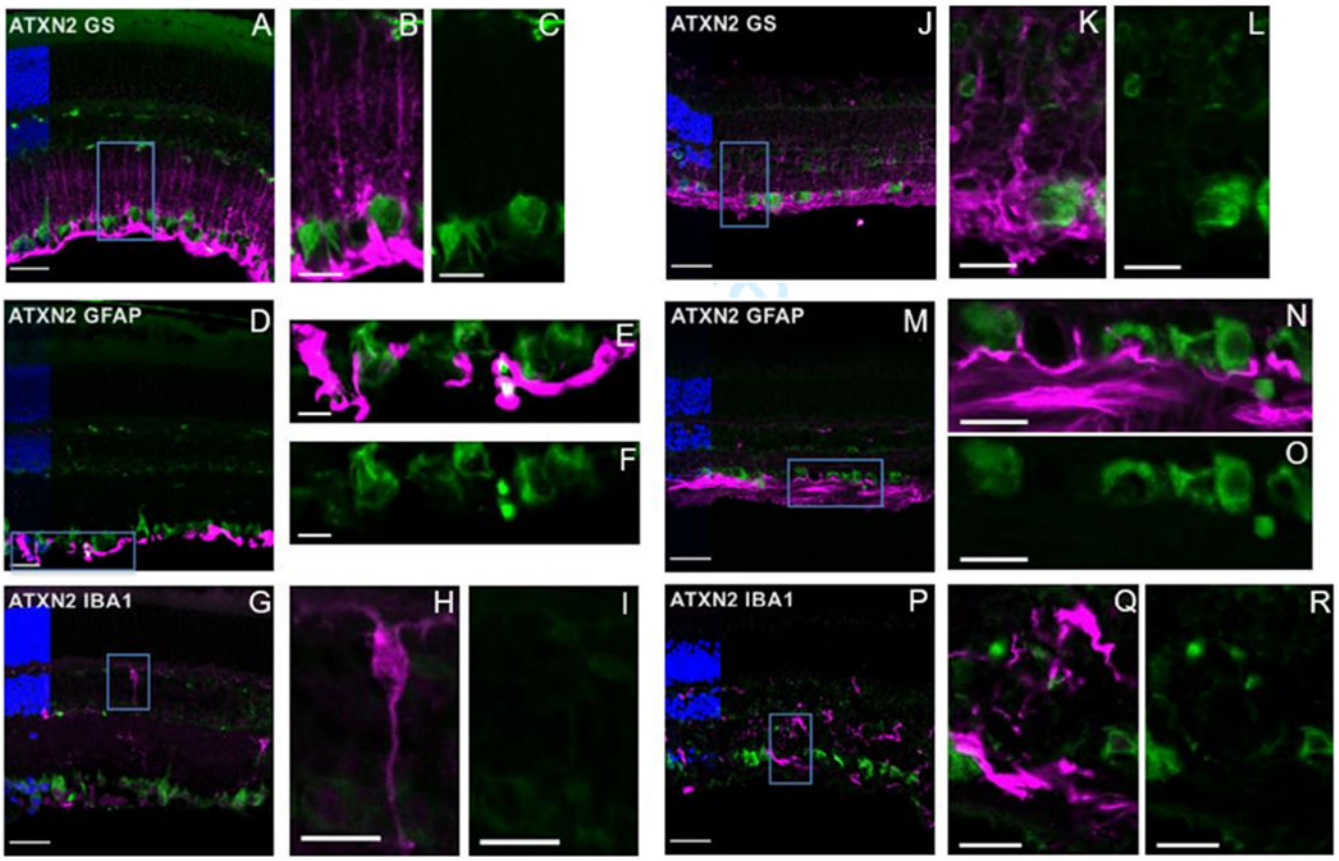


**FIGURE 5.**

Mouse (a–i) and human retina (j–r) were investigated for co-localization of ATXN2 with markers of retinal glia such as Müller cells (GS), astrocytes (GFAP), and microglia (IBA1). There was no indication of co-localization between ATXN2 and any glial markers in mouse or human tissues. Scale bars: 25 μm (a,d,g,j,m,p) and 10 μm (b,c,e,f,h,i,k,l,n,o,q,r) [Color figure can be viewed at wileyonlinelibrary.com]

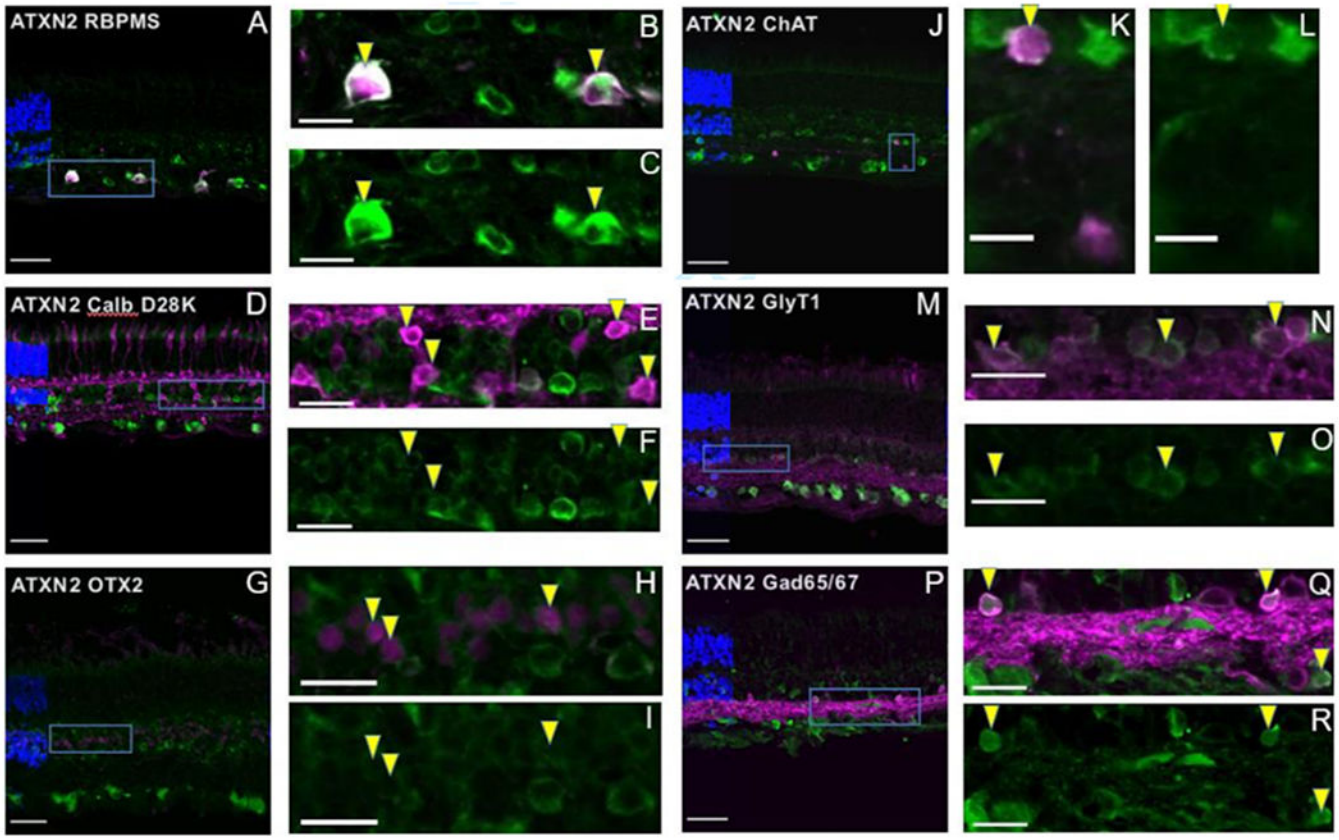


**FIGURE 6.**

Human tissue was co-labeled for ATXN2 (green) and markers (magenta) for RGCs (RBPMS; a–c), amacrine cells (ChAT, GlyT1, GAD 65/67; j–r), horizontal cells (Calb D28K; d-f), and bipolar cells (OTX2; g–i). Findings from human tissue agree with those from mouse tissue indicating that ATXN2 expression is highest in RGCs and amacrine cells. ATXN2-ir is detected in horizontal cells and potentially bipolar cells. Enlarged insets show merged channels and ATXN2-specific immunofluorescence with yellow arrowheads indicating colocalization of ATXN2 with cell type-specific markers. Scale bars: 25 μm (a,d,g,j,m,p) and 10 μm (b,c,e,f,h,i,k,l,n,o,q,r) [Color figure can be viewed at wileyonlinelibrary.com]

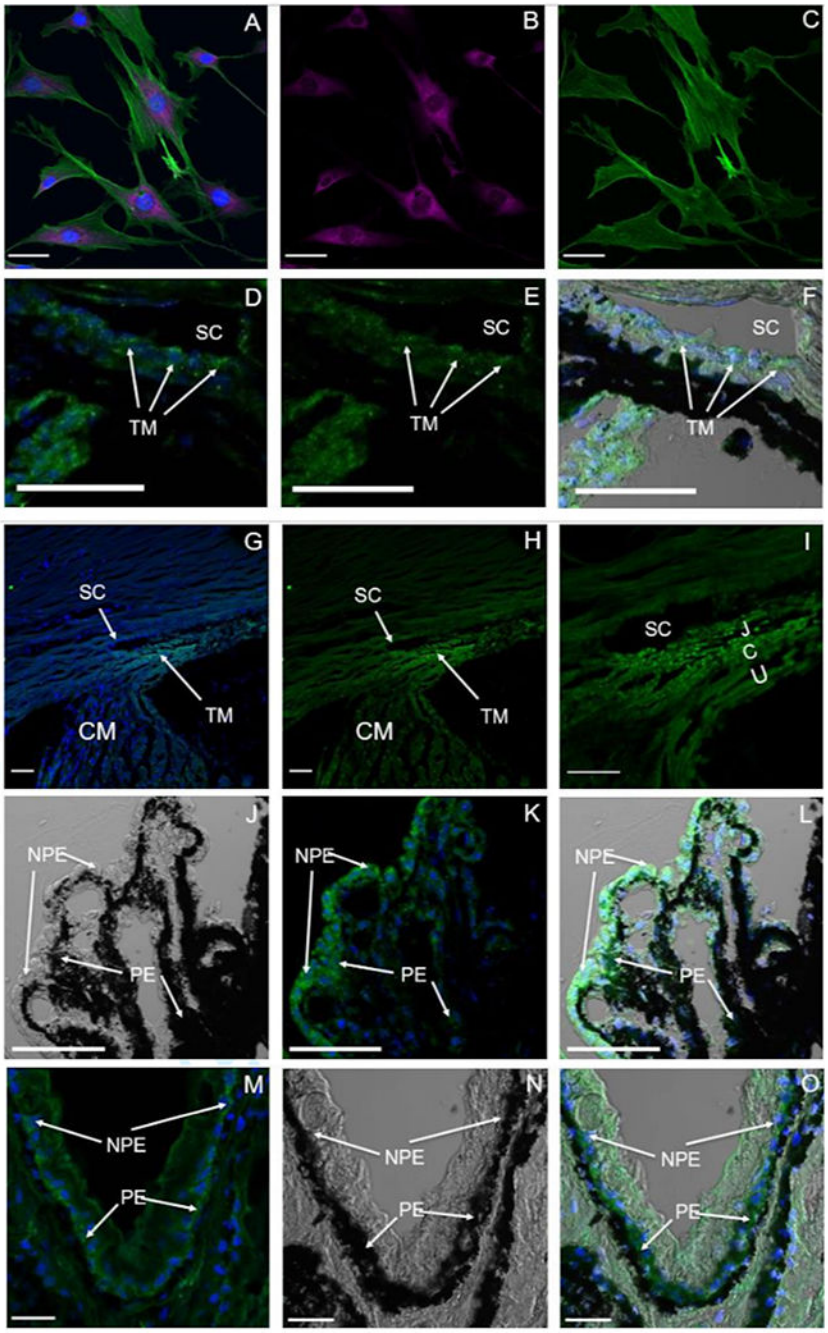


**FIGURE 7.**

(a-c) Primary human trabecular meshwork cells show ATXN2-ir (FITC) in the cytoplasm and the perinuclear region. (d-i) The ATXN2 antibody labels mouse and human TM tissue butnot the endothelial cells of the Schlemm's canal (SC). (g-i) Human TM. ATXN2-ir is seen in juxtacanalicular (J) and corneoscleral (C) regions, but lower signal in the uveoscleral (U) region. Nonpigmented (NPE) and pigmented epithelium (PE) of the ciliary body in

mouse j–l) and human tissues (m–o) are ATXN2-ir. Scale bars: 25 μm [Color figure can be viewed at wileyonlinelibrary.com]

**TABLE 1**

Primary antibodies

| Antibody target | Description of immunogen | Company name | Mono/polyclonal | Source | IHC dilution |
|---|---|---|---|---|---|
| ATXN2 | 713-904 amino acid sequence of the Human Ataxin-2 | BD Transduction Laboratories (611,738; RRID: AB_398900) | Monoclonal | Mouse | 1:300 |
| ATXN2 | Custom-designed against the EKSTESSSGPKREE epitope sequence common to both humans and mice | Custom | Polyclonal | Rabbit | 1:300 |
| RBPMS | Synthetic N-terminal peptide of the rat RBPMS sequence | PhosphoSolutions (1830-RBPMS; RRID: AB_2492225) | Polyclonal | Rabbit | 1:500 |
| GFAP | GFAP protein isolated from cow spinal cord | Agilent DakoCytomation (Z0334; RRID: AB_10013382) | Polyclonal | Rabbit | 1:500 |
| GAD 65/67 | Against C-terminal sequence (a.a. 423–585) of purified protein from rat brain | Developmental Studies Hybridoma Bank GAD-6-s (AB_2314499) | Monoclonal | Mouse | 1:50 |
| GlyT1 | Synthetic C-terminal peptide from rat serum | EMD Millipore (AB1770; RRID: AB_90893) | Polyclonal | Goat | 1:1000 |
| ChAT | Human placental peptide | EMD Millipore (AB144-P; RRID: AB_2079751) | Polyclonal | Goat | 1:300 |
| Calb D28K | Recombinant mouse peptide | EMD Millipore (AB1778; RRID: AB_2068336) | Polyclonal | Rabbit | 1:100 |
| OTX2 | Human Otx2 Met1-Leu289 | R&D Systems (AF1979; RRID: AB_2157172) | Polyclonal | Goat | 1:1000 |
| IBA1 | Synthetic peptide (proprietary) | Abcam (ab178846; RRID: AB_2636859) | Monoclonal | Rabbit | 1:2000 |
| GS | C-terminal portion of human peptide | Santa Cruz (SC-6640; RRID: AB_641095) | Polyclonal | Goat | 1:100 |